INFORMATION TO USERS

This manuscript has been reproduced from the microfilm master. UMI films the text directly from the original or copy submitted. Thus, some thesis and dissertation copies are in typewriter face, while others may be from any type of computer printer.

The quality of this reproduction is dependent upon the quality of the copy submitted. Broken or indistinct print, colored or poor quality illustrations and photographs, print bleedthrough, substandard margins, and improper alignment can adversely affect reproduction.

In the unlikely event that the author did not send UMI a complete manuscript and there are missing pages, these will be noted. Also, if unauthorized copyright material had to be removed, a note will indicate the deletion.

Oversize materials (e.g., maps, drawings, charts) are reproduced by sectioning the original, beginning at the upper left-hand corner and continuing from left to right in equal sections with small overlaps.

ProQuest Information and Learning
300 North Zeeb Road. Ann Arbor, MI 48106-1346 USA
800-521-0600

Université d'Ottawa • University of Ottawa

EVIDENCE FOR THE PRESENCE OF LARGE-SCALE DELETION MUTATIONS IN A MURINE TUMOUR MODEL

Sherry Weppler

A thesis submitted to
the Faculty of Graduate and Postdoctoral Studies
in partial fulfillment of the requirements for the degree of
Master of Science

Department of Biochemistry, Microbiology and Immunology

University of Ottawa
Ottawa, Ontario. Canada

ABSTRACT

Genomic instability of cancer cells is a well documented feature of tumour progression. In addition to endogenous factors in tumour cells, exogenous factors present within the tumour environment may also contribute to this genotoxicity. Inflammatory cells, often found infiltrating solid tumours, produce reactive nitrogen and oxygen radicals, which may be genotoxic. Thus, providing evidence of mutagenicity associated with inflammatory cells could help to explain the known association between chronic inflammation and increased cancer risk.

In order to study mutagenicity occurring within a tumour environment, our lab has developed the Mutatect murine tumour model, which is able to sensitively detect mutations at a genetically manipulated hprt locus. Prior to my work, the X-linked hprt gene in the Mutatect cell lines was thought to be heterozygous based on high sensitivity to induction of mutations by ionizing radiation and the identification of 3 X-chromosomes by fluorescent *in situ* hybridization. In order to determine the hprt genotype and to confirm that the hprt gene was indeed heterozygous, the hprt cDNA of Mutatect cells was cloned and sequenced. Three mRNA species were identified: mRNA-A corresponds to wild type hprt, mRNA-B contains a single nucleotide deletion within exon 3, and mRNA-C contains a deletion of exons 2 and 3.

Previous experiments with the Mutatect tumour model have shown an increase in mutation frequency associated with *in vivo* growth and increasing numbers of infiltrating neutrophils within the tumour environment. In order to

identify the types of mutations that are generated during *in vivo* tumour growth, a screening method was devised to analyze mutations occurring in the wild type hprt gene. This strategy involves sequencing of RT-PCR products over the region in exon 3 that is unique to each hprt mRNA, and will identify mutations that prevent expression of the wild type mRNA-A. Using this technique, a series of *in vitro* spontaneous and X-ray induced, and *in vivo* spontaneous and glyceryl trinitrate-induced mutants were examined. All mutants showed an absence of the wild type sequence, consistent with the hypothesis that large-scale deletions are induced in Mutatect cells by these treatments. This study supports the suggestion that mutagenic factors present in the tumour microenvironment contribute to genotoxicity through the production of large-scale deletion mutations.

ACKNOWLEDGEMENTS

I would like to thank my supervisor, Dr. Birnboim, for giving me the oppurtunity to work on this challenging project. I would also like to express my thanks to the other members of my thesis advisory committee, Dr. D. Bulman, Dr. R. Walker, and Dr. B. Wouters, for their guidance and helpful suggestions. Special thanks to Dr. Bulman for allowing me to run the sequencing gels in his lab, and to Dr. J. Sandhu for generating the glyceryl trinitrate mutants.

I would like to express my appreciation to Donna Grant and Denise Proulx for their excellent technical assistance with the mouse experiments, as well as to the other members of the Birnboim lab for all their help and encouragement. Lastly, but certainly not least, I would like to thank Dr. R. Chiu and Jan Brun for their undying support, especially through the editting process.

TABLE OF CONTENTS

LIST OF TABLES

LIST OF FIGURES

LIST OF ABBREVIATIONS

6-TG	6-thioguanine
6-TG^R	6-thioguanine resistant
6-TG^S	6-TG sensitive
aprt	adenine phosphoribosyl transferase
BER	base excision repair
bp	base pair
CDTA	1,2-cyclohexanediaminetetraacetic acid
ddNTP	dideoxynucleotide
DEPC	diethyl pyrocarbonate
DMEM	Dulbecco's modified Eagle medium
DTT	dithiothreitol
ecNOS	endothelial cell NOS
EMS	ethyl methanesulfonate
FCS	fetal calf serum
FISH	flourescent *in situ* hybridization
Gy	Gray
GTN	Glyceryl trinitrate
H_2O_2	hydrogen peroxide
HAT	hypoxanthine-aminopterin-thymidine
HAT^R	HAT resistant
HIF-1	hypoxia-inducible factor-1

HRE	hypoxia-response element
IEC	International Equipment Company
iNOS	inducible nitric oxide synthase
Kb	kilobasepairs
MNU	N-methyl-N-nitrosourea
N_2O_3	nitrous acid
nNOS	neuronal NOS
NO	Nitric oxide
NO_3^-	nitrate
NOS	nitric oxide synthase
O_2^-	superoxide anion
$OONO^-$	peroxynitrite
PARP	poly(ADP-ribose) polymerase
PBS	phosphate buffered saline
PEG	polyethyleneglycol
RNOS	reactive nitrogen oxide species
RT-PCR	reverse transcriptase-polymerase chain reaction
SDS	sodium dodecylsulfate
TNF-α	tumour necrosis factor-α
UV	ultraviolet
VEGF	vascular endothelial growth factor
X-Gal	5-bromo-4-chloro-3-indolyl-β-D-galactoside

1. GENERAL INTRODUCTION

1.1 Genomic instability and carcinogenesis

Cancer is a multi-stage disease whereby somatic cells acquire an increasingly proliferative and invasive behaviour through the accumulation of mutations. Numerous genetic alterations have been observed in neoplastic cells, including gross chromosomal aberrations (i.e., large-scale deletions, rearrangements, gene amplifications, aneuploidy), as well as sequence alterations (i.e., point mutations, small deletions and insertions) (Coleman and Tsongalis, 1999). As tumours progress from a benign to a metastatic stage, they often acquire an increasing number of these genetic alterations. Thus, genomic instability has been suggested to play a vital role in the initiation and progression of tumours (Coleman and Tsongalis, 1999).

Knudson's two-hit hypothesis proposes that at least two mutations are required for the initiation of carcinogenesis (Knudson, Jr., 1977). In his study of inherited retinoblastoma, he proposed that a genetic predisposition was conferred if an individual inherited a germline mutation, and that a second "hit" (i.e., somatic mutation) was required in the remaining allele in order for cancer to develop. While this model holds true for some tumour types, it is now generally recognized that the progression of cancer requires mutational events to occur at multiple sites, including both oncogenes and tumour suppressor genes. For example, in a model of colorectal cancer, 4-5 different chromosomal rearrangements have been identified that correlate with the well-defined histopathologic stages of tumour progression (Fearon and Vogelstein, 1990).

A model of tumour progression based on genetic instability and clonal selection, proposed by Nowell, suggests that each mutational event is followed by selection for increased proliferative potential (Nowell, 1976). Thus, the first advantageous mutation will lead to the limited expansion of a single cell, and each subsequent mutation has the possibility of producing a clonal outgrowth with greater proliferative capabilities.

The large number of mutations found in tumours cannot be explained by the spontaneous rate of mutation observed in normal somatic cells. In order to explain this phenomenon, Loeb has suggested the induction of a "mutator phenotype" early in tumour development (Loeb, 1991). He proposes that mutational inactivation of a gene required for the maintenance of genomic stability would promote the acquisition of many more mutations elsewhere in the genome. Maintenance of genomic stability is thought to involve proteins participating in DNA replication, DNA repair pathways, cell cycle check points, and chromosome partitioning during cell division (Loeb, 1991).

In addition to these endogenous factors, which are postulated to play a role in genetic instability, exogenous factors present within the tumour microenvironment may also contribute to mutagenesis. The solid tumour microenvironment consists of not only tumour cells, but also immune cells and endothelial cells that form the tumour vasculature. These components in combination produce an environment characterized by fluctuating oxygen levels, low pH, and nutrient deprivation (Yuan and Glazer, 1998). Several animal models have shown an increase in mutation frequency induced by the tumour

environment (Wilkinson et al., 1995), suggesting that mutagenic factors are present and may be acting through the induction of mutagenic lesions and/or through the inhibition of DNA repair. Supporting this hypothesis is evidence that cells in culture, when exposed to hypoxia and low pH, have a compromised DNA repair ability (Yuan et al., 2000).

1.2 Mutatect tumour model system

The Mutatect tumour model was developed in order to examine the mutagenic potential of the tumour microenvironment, with hopes of identifying tumour-associated factors that could contribute to genomic instability and tumour progression. This model system consists of a series of murine fibrosarcoma cell lines that have been genetically altered at the X-linked hprt locus to allow for the sensitive detection of both small and large-scale mutational events. Mutatect cells are transplantable by subcutaneous injection into syngeneic C57Bl/6 mice where they form a malignant tumour after 2-3 weeks (Figure 1-1). These cells utilize the hprt gene as a marker to detect mutations that occur during *in vivo* or *in vitro* growth. After tumour excision, the Mutatect cells can be cultured *ex vivo* in selective media containing 6-thioguanine (6-TG) in order to select for hprt mutants.

1.3 Advantages provided by the Mutatect system

The Mutatect system offers several advantages in its ability to detect mutational events occurring *in vivo*. These cells employ an endogenous marker

Figure 1-1. The Mutatect tumour model.

Mutatect tumour cells are injected by subcutaneous injection into the hind flank of a syngeneic C57Bl/6 mouse. Tumour formation occurs over a 2-3 week period, during which time various experimental treatments can be delivered. After the tumour is removed, the cells are cultured *ex vivo* in selective medium to determine the mutation frequency at the hprt marker locus.

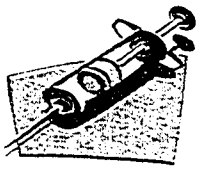

Subcutaneous injection of Mutatect cells

C57Bl/6

Allow 2-3 weeks for tumour to form

Tumour excision

6-TG

→ Culture cells *ex vivo* to allow hprt$^-$ colonies to form

→ Count colonies to determine mutation frequency

gene, rather than a foreign exogenous marker gene that has been integrated into the genome. Transfected marker genes tend to be problematic since inactivation of the transgene can occur at a very high frequency (1-5%) (Gebara et al., 1987), thus leading to a much higher spontaneous rate of mutation than for an endogenous locus. A high spontaneous mutation frequency also makes detection of induced mutations more difficult.

Endogenous marker genes can be of two types: hemizygous or heterozygous. A hemizygous marker gene is present in a single copy within a diploid genome, whereas a heterozygous gene has two or more unique alleles. In mammalian cells, the hprt gene is functionally hemizygous due to the presence of only one X-chromosome in males, and due to the process of X-inactivation in females. During the development of the Mutatect cell lines, however, we believe that the hprt locus has been altered to heterozygosity (see Ch.2). In order to sensitively detect large-scale multi-locus mutations, it is advantageous to use a heterozygous marker (DeMarini et al., 1989). A large deletion mutation that eliminates a large portion of a chromosome may also remove neighbouring essential genes. If this is the case, at a hemizygous marker locus this mutant would not be viable, and thus, would not be scored during calculation of the mutation frequency. However, if the marker gene is heterozygous, the homologous chromosome is able to provide the essential sequences required for growth of the mutant cell.

The physical location of the marker gene also plays a role in the ability of a system to detect clastogenic events. The distance of the marker gene from an

adjacent essential gene determines the size and number of large-scale mutations that will be recovered. Thus, the spectrum of mutations induced by the same agent may vary markedly between two different genetic loci. Ionizing radiation has been shown to induce substantial deletions at the hprt locus, which also affect large neighboring regions of the genome. In comparison, the adenine phosphoribosyl transferase (aprt) locus demonstrates no detectable alterations in gene structure (Breimer et al., 1986). The human hprt gene is predicted to be 2-3 Mb from an essential gene, towards the centromere of the X-chromosome (Wu et al., 1998). Large deletions of up to 2.8 Mb have been recovered at the human hprt locus (Phillips et al., 1995). Therefore, the Mutatect system should be capable of detecting large-scale mutations occurring at this locus.

1.4 Previous findings provided by the Mutatect model

Previous experiments using the Mutatect system have shown that the mutation frequency of MN-11 cells (one of the Mutatect fibrosarcoma cell lines) grown as a tumour is 3.4 fold higher than cells grown in tissue culture (Sandhu et al., 2000a). This result suggests that exogenous mutagenic factors are present within the tumour environment. Histochemical analysis of tumour sections revealed a poorly differentiated fibrosarcoma that was very vascular. A large number of infiltrating neutrophils were identified near the blood vessels and in necrotic areas, and to a lesser extent at the tumour periphery. Occasional lymphocytes, macrophages, and mast cells were also identified at the tumour periphery. In a more recent experiment with the Mutatect model, a positive

correlation was found between the mutation frequency of tumours and the number of infiltrating neutrophils (Sandhu et al., 2000a).

1.5 Nitric oxide and the tumour microenvrionment

Nitric oxide (NO) is believed to be present within the tumour environment as a by-product of infiltrating immune cells. Immunohistochemical staining of MN-11 tumour sections showed that tumour-associated neutrophils expressed inducible nitric oxide synthase (iNOS), the enzyme responsible for the production of nitric oxide (Sandhu et al., 2000b). The iNOS produced by the neutrophils appears to be active, as tumour homogenates display NOS activity when assayed *in vitro*. The NOS activity of tumour homogenates was also positively correlated with mutation frequency. Thus, elevated levels of nitric oxide within the tumour microenvironment may play a role in the genetic instability observed during *in vivo* tumour growth.

1.6 Biosynthesis of nitric oxide

Nitric oxide is generated by the enzyme nitric oxide synthase (NOS), which catalyzes the conversion of L-arginine to L-citrulline (Figure 1-2). Three different isoforms of NOS, encoded by individual genes located on separate chromosomes, have been characterized: endothelial cell NOS (ecNOS), neuronal NOS (nNOS), and inducible NOS (iNOS). Both ecNOS and nNOS are constitutively expressed, but their enzyme activity is induced, via binding of

Figure 1-2. Synthesis of nitric oxide and its genotoxic effects.

Nitric oxide synthase catalyzes the conversion of L-arginine to L-citrulline and nitric oxide, in the presence of oxygen and NADPH. The bottom portion of the figure illustrates the downstream reactions of nitric oxide with oxygen and superoxide anion. These reactive molecules bring about the genotoxic effects of nitric oxide through interactions with DNA, nucleosides, and DNA repair enzymes.

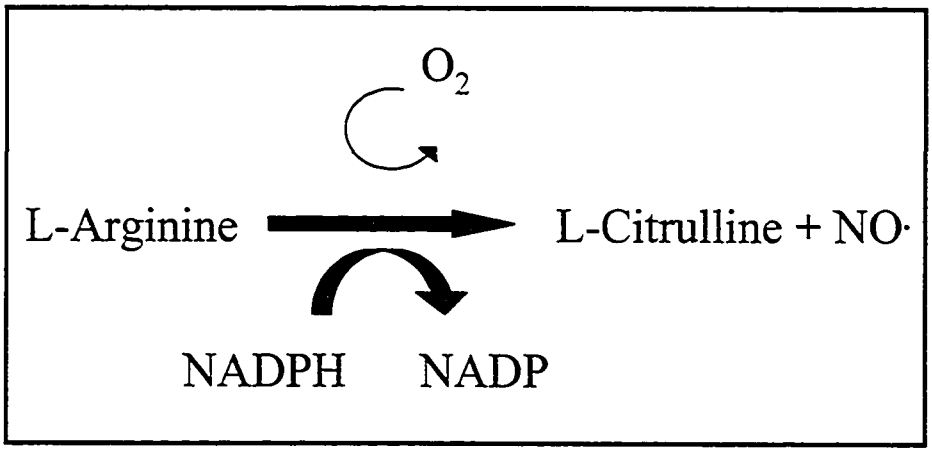
O2
L-Arginine
L-Citrulline + NO·
NADPH
NADP

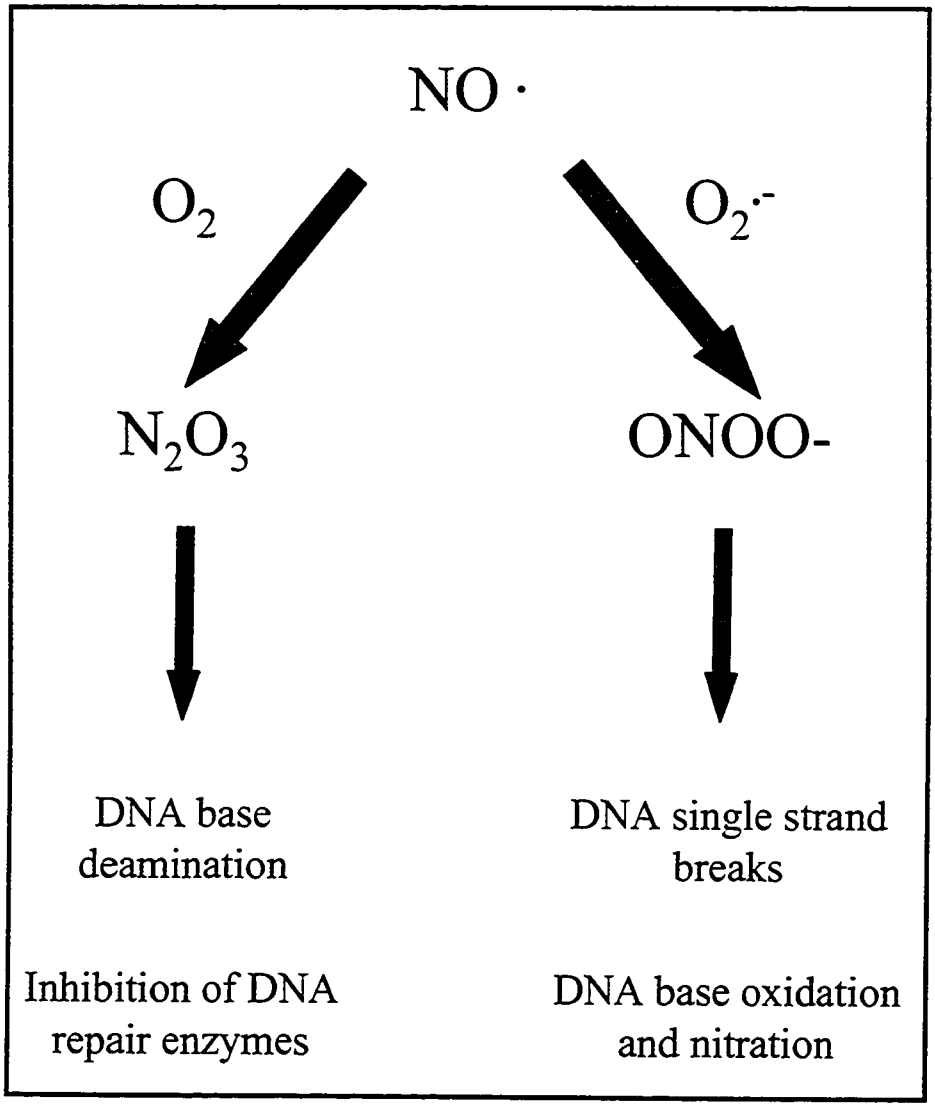
NO ·
O2
O2·-
N2O3
ONOO-
DNA base deamination
DNA single strand breaks
Inhibition of DNA repair enzymes
DNA base oxidation and nitration

calmodulin, by elevated levels of intracellular calcium (Bruch-Gerharz et al., 1998). These isoforms are responsible for producing low picomolar concentrations of NO for short periods of time, a requirement for the processes of neurotransmission and vasodilation (Nathan, 1992). In this context, NO plays a role in cellular signalling through its molecular target, soluble guanylate cyclase. The inducible isoform is transcriptionally regulated by various cytokines (interferon-γ, tumour necrosis factor-α, interleukin-8, and interleukin-1β) and lipopolysaccharide. Furthermore, iNOS activity is calcium-independent (Dugas et al., 1995). iNOS is able to produce large nanomolar concentrations of NO for sustained periods of time, lending to its importance in immune defense and regulation of the immune response. During the inflammatory response against invading pathogens, macrophages and neutrophils secrete NO in combination with other species, such as superoxide anion (O_2^-) and hydrogen peroxide (H_2O_2) (Hibbs, Jr. et al., 1988). Although beneficial to host defense, the cytotoxicity of NO becomes harmful in situations of chronic inflammation where high levels of NO are produced over months or even years. Inappropriate expression of iNOS has been implicated in a number of inflammatory and autoimmune diseases such as lupus erythematosus, Crohn's disease, rheumatoid arthritis, and diabetes (Eizirik and Leijerstam, 1994). Hence, due to its beneficial as well as detrimental roles, NO has often been described as a double-edged sword.

1.7 Modulation of proteins by nitric oxide

NO is a small, uncharged molecule that can easily diffuse across lipid membranes. The biological lifetime is between 5-10 seconds due to its rapid reactions with oxygen and oxyhemoglobin. In the latter reaction, NO binds to the heme ring and oxidizes Fe^{2+} to form met-hemoglobin and nitrate (NO_3^-) (Ignarro et al., 1993). Due to the high concentration of oxyhemoglobin in blood and the rapid rate of this reaction, nitrate is the major endpoint metabolite of NO *in vivo* (Beckman and Koppenol, 1996). This pathway can be thought of as a detoxification mechanism, by promoting the production of nitrate rather than other more harmful reactive nitrogen oxide species (RNOS).

In a similar fashion, NO is able to covalently bind to iron-sulfur (Fe-S) centers, often found in enzyme active sites, to form a Fe-nitrosyl complex (Wink and Mitchell, 1998) by the following reaction:

$$Fe(II) + NO \rightarrow Fe(II)—NO$$

Hence, nitric oxide is able to inhibit protein function by prevention of substrate binding. Proteins that can be inactivated in this way include cytochrome P450, cytochrome oxidase, and catalase.

There is evidence to suggest that NO can alter gene expression by inhibiting the action of various transcription factors. NO is able to prevent the binding of SP-1, a transcriptional repressor in this case, to the TNF-α promoter, resulting in an increase of tumour necrosis factor-α expression (Wang et al.,

1999). The expression of vascular endothelial growth factor (VEGF) is also regulated by NO by way of a cis-acting NO-response element in its promoter region. This element has been shown to co-localize to the hypoxia-inducible factor-1 (HIF-1) binding site within the hypoxia-response element (HRE), thus suggesting that NO and hypoxia may share common features in the pathway of VEGF induction (Kimura et al., 2000). A mechanism involving the removal of zinc ions, by nitrosylation of adjacent thiol groups, would allow NO to inhibit the DNA-binding activity of zinc-finger type transcription factors (Bruch-Gerharz et al., 1998).

1.8 Genotoxicity of nitric oxide

NO alone is not considered to be mutagenic, but through its interactions with oxygen and superoxide anion, it generates reactive molecules (N_2O_3 and $ONOO^-$ respectively) which have been documented to be genotoxic (Figure 1-2). NO, under aerobic conditions, is able to deaminate purine and pyrimidine bases resulting in base pair substitutions and single-strand breaks (Nguyen et al., 1992). The chemical species responsible for this damage is thought to be nitrous acid (N_2O_3), the predominant nitrosating agent arising from NO at physiological pH (Felley-Bosco, 1998). The following reactions describe the formation of N_2O_3:

$$2\ NO + O_2 \rightarrow 2\ NO_2$$

$$NO_2 + NO \rightarrow N_2O_3$$

The consequences of nucleoside deamination are dependent upon the nucleoside structure. For example, deamination of guanine yields xanthine, which can readily depurinate to form an abasic site in DNA (Burney et al., 1999). Endonucleases may cleave this site resulting in production of a single-strand break. Alternatively, DNA polymerase may replicate past the abasic site by inserting adenine opposite this position, thus leading to a G:C → A:T transversion mutation. In contrast, deamination of 5-methylcytosine to thymine simply results in a G:C → A:T transition.

When NO and O_2^- are temporally and spatially co-produced, as is often the case during inflammatory reactions, the powerful oxidant peroxynitrite ($OONO^-$) is formed. Peroxynitrite can initiate a number of DNA base modifications *in vitro*, including the production of 8-oxoguanine and 8-nitroguanine. The presence of 8-oxoguanine in DNA is known to cause G:C→A:T transitions (Burney et al., 1999), while 8-nitroguanine is rapidly depurinated, suggesting that it may be responsible for the production of G:C → T:A transversions through the production of abasic sites (Yermilov et al., 1995). 8-nitroguanine is especially significant as its production has been attributed solely to $OONO^-$, and no other mutagenic agents, therefore it may provide a measure of $OONO^-$-specific DNA damage (Szabó and Ohshima, 1997).

In addition to the oxidation or nitration of DNA bases, $OONO^-$ can cause mutations by the production of single strand breaks. $OONO^-$ can trigger strand breakage either directly by reaction with the sugar moiety of DNA, thus inducing its fragmentation and subsequent strand breakage, or indirectly by way of

unstable base modifications (Burney et al., 1999). The accumulation of strand breaks in DNA causes the activation of poly(ADP-ribose) polymerase (PARP). This enzyme repeatedly transfers ADP-ribose from NAD+ to various nuclear proteins, forming an ADP-ribose polymer of up to 100 units in length. Major protein acceptors of poly(ADP-ribose) include DNA polymerases α and β, topoisomerase I and II, and DNA ligase 2 (Szabó and Ohshima, 1997). ADP-ribosylation of proteins generally results in a decrease in their catalytic activities. Sustained activation of PARP rapidly depletes the cell's NAD+ supply, therefore leading to a decrease in ATP formation, and possibly even cell death (Murphy, 1999). PARP knockout mice have provided recent evidence that PARP is involved in the DNA synthesis step of base excision repair (BER) (Dantzer et al., 1999).

Also contributing to NO-induced genotoxicity is the ability of RNOS to inhibit the activity of DNA repair proteins. In particular, DNA ligase activity is inhibited through nitrosation of a partially deprotonated lysine residue in the enzyme active site (Graziewicz et al., 1996). Thus, inhibition of DNA ligase may promote the accumulation of DNA breaks formed by the actions of RNOS and $OONO^-$

1.9 Evidence of large-scale deletions produced by nitric oxide

Previous studies in our lab employing a human B-lymphoblastoid cell line, WIL2-NS, have shown that nitric oxide donating drugs are capable of causing large-scale deletion mutations (Grant, 1999). Mutant hprt clones were collected,

and characterized by multiplex-PCR over all nine exons and two flanking marker sequences (DXS79 and DXS86). Large-scale deletions were identified by failure to amplify one or more PCR fragments. By this method, 60-81% (depending on the drug used) of the mutant clones isolated displayed large-scale deletions at the hprt locus compared to 11% of spontaneously generated mutants. The spontaneous mutants all failed to amplify a single exon (exon 9), whereas the majority of the nitric oxide induced mutations involved multiple exon deletions ranging in size from 2.6 Kb to >1.2 Mb. To our knowledge, this is the first evidence that nitric oxide is involved in producing mutations of this magnitude.

1.10 Hypothesis

We hypothesize that mutagenic factors present in the tumour microenvironment can contribute to genomic instability through the induction of large-scale deletion mutations within tumour cell DNA.

1.11 Objective

To determine whether large-scale deletion mutations can be observed in Mutatect cells as a result of *in vivo* tumour growth.

2. MOLECULAR CHARACTERIZATION OF THE HPRT GENOTYPE OF MUTATECT CELLS

2.1 Introduction

2.1.1 Hprt gene as a marker of mutational events

The hprt gene has been widely used for studies of mammalian cell mutagenesis. This gene is commonly used as a genetic marker of mutational events since cells containing mutant hprt protein can easily be selected by growth in media containing 6-TG, a purine analog (Chinault and Caskey, 1984). The Hprt enzyme catalyzes the conversion of hypoxanthine and guanine to their respective 5' mononucleotides, thus participating in the purine salvage pathway whereby exogenous purines are metabolized and incorporated into newly synthesized DNA (Rincon-Limas et al., 1991). Hprt metabolizes 6-TG to a toxic intermediate; thus cells that have a mutant hprt protein will be resistant to the effects of 6-TG since they are unable to use the salvage pathway. HAT (hypoxanthine-aminopterin-thymidine) selection works in the opposite way; since aminopterin blocks *de novo* purine synthesis, only $hprt^+$ cells, which can rely on the salvage pathway, are able to survive.

The murine hprt gene is located on the X-chromosome and is composed of nine exons which span a distance of ~33 kilobasepairs (Kb) (Melton et al., 1984). The relatively small exons, ranging in size from as few as 18 bp to 593 bp, are interspersed between large introns and are transcribed to form an mRNA of 1307 bp (Figure 2-1). Approximately half of the message (654 bp) comprises the protein-coding region since a large portion of exon 9 contains untranslated

Figure 2-1. Murine hprt gene structure.

The mouse hprt gene is comprised of nine exons that span 33 Kb of the X-chromosome. Exon sizes are indicated in number of base pairs, while introns are indicated in kilobase pairs. Shaded regions correspond to the untranslated portions of exons 1 and 9.

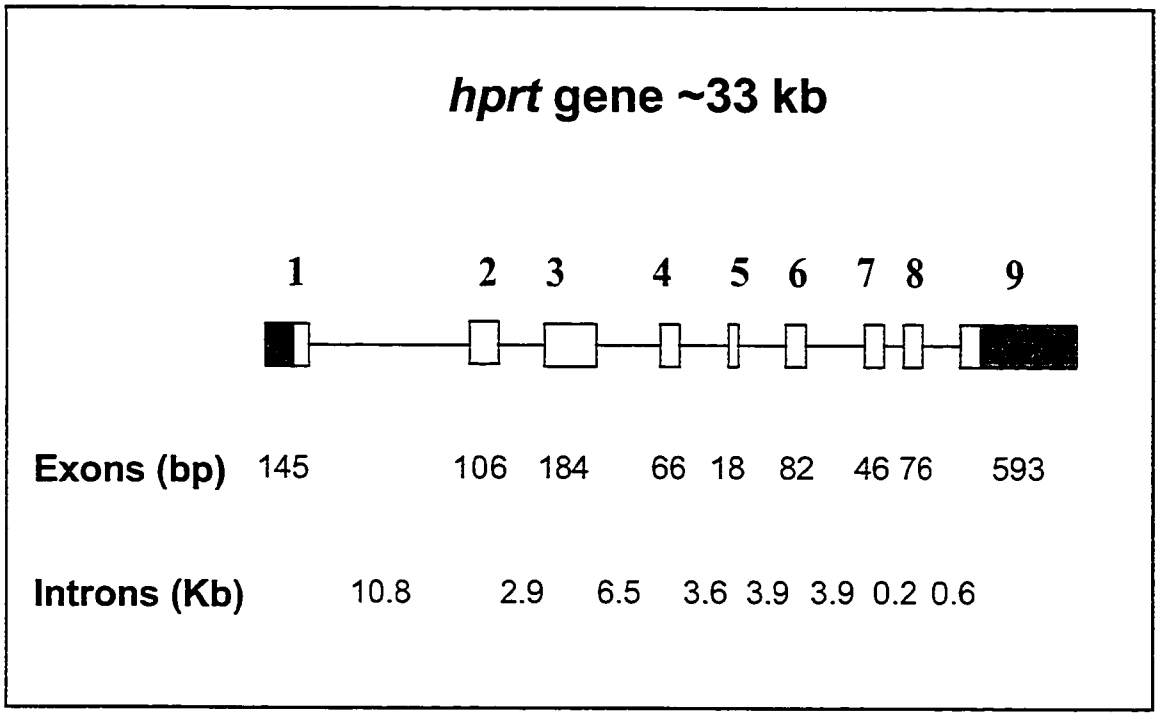
hprt gene ~33 kb
1 2 3 4 5 6 7 8 9
Exons (bp) 145 106 184 66 18 82 46 76 593
Introns (Kb) 10.8 2.9 6.5 3.6 3.9 3.9 0.2 0.6

sequence. In addition to the functional X-linked gene, a mouse hprt pseudogene also exists. It is a processed pseudogene that comprises the complete reverse transcript of the mRNA with the exception of a small internal 89 bp deletion (Isamat et al., 1988). The mouse pseudogene has been located to the distal end of chromosome 17 and does not appear to have homology to any of the multiple human hprt pseudogenes.

The hprt gene is a housekeeping gene that is constitutively expressed in all tissues at a low level, with the exception of brain where the enzyme activity is approximately seven-fold higher than in other tissues (Chinault and Caskey, 1984). Similar to other housekeeping genes, it lacks TATA and CAAT boxes in the promoter region, but instead contains a series of highly G/C rich direct repeats that are required for expression (Melton et al., 1986). A negative regulatory element present in the 5'-flanking sequences may be involved in the tissue-specific level of expression (Rincon-Limas et al., 1991). Although the hprt enzyme is not considered to be essential for cell viability, at the systemic level partial hprt deficiency is associated with gouty arthritis while complete hprt deficiency leads to the neurological disorder known as Lesch-Nyan syndrome. Due to the seriousness of the latter disease, many hprt mutations that abrogate expression of a functional enzyme have been identified (Stout and Caskey, 1988).

2.1.2 Development of Mutatect cell lines

The Mutatect tumour model system was developed over several years, and is comprised of numerous cell lines that have been manipulated in order to allow for the sensitive detection of mutations at the hprt locus (Wilkinson et al., 1995) (Figure 2-2). Parental Mutatect tumour cells were isolated from a fibrosarcoma that had been chemically induced using methylcholanthrene, a powerful carcinogen, in a male C57Bl/6 mouse. This tumour was known to be infiltrated with inflammatory cells and could be readily transplanted as tumour fragments in syngeneic animals (Kadhim et al., 1987). The tumour was excised and the cells were used to establish a tissue culture line designated MC1A-C1. In order to inactivate the hprt marker gene(s), these cells were treated with the chemical mutagen N-methyl-N-nitrosourea (MNU). It proved difficult to obtain 6-thioguanine resistant (6-TG^R) colonies following this treatment, thus suggesting that more than one functional copy of the hprt gene was present. One of the few 6-TG^R clones that arose, designated MC-TGR17, was selected for further manipulation based on its continued ability to form subcutaneous tumours in mice. The final step in the development of this system was to reactivate one of the hprt genes to allow for its use as a marker of mutational events. MC-TGR17 was cultured in HAT medium until several spontaneous revertants arose which were both HAT resistant (HAT^R) and 6-TG sensitive (6-TG^S). A HAT^R clone, designated MC-TGS17-51, was selected for future work based upon its stable hprt expression (i.e., lowest spontaneous reversion to 6-TG resistance). MN-11 is a derivative of MC-TGS17-51 in which the cDNA for neomycin resistance was

Figure 2-2. Derivation pathway of Mutatect cell lines.

Mutatect cells were isolated from a C57Bl/6 fibrosarcoma and were subsequently altered at the hprt locus to allow for the sensitive detection of mutations during both *in vitro* and *in vivo* growth. The hprt phenotype, as well as the suspected genotype, of each cell line in the pathway is indicated.

C57BL/6

MC1A (3-X chromosomes)

MC1A-C1 (Capable of *in vitro* growth)

MNU

MC-TGR17 (6-TG^R ; hprt -)

Spontaneous reversion

MC-TGS17-51 (6-TG^S ; hprt +)

Neo gene

IL-8 gene
Neo gene
Hyg gene

MN-11

(6-TG^S ; hprt +)
(G418^R)

TM-28

(6-TG^S ; hprt +)
(G418^R, Hyg^R)

introduced using a retroviral vector, thus allowing the Mutatect tumour cells to be readily distinguished from host cells after tumour excision. Another derivative of MC-TGS17-51, TM-28, was developed in order to increase the attraction of neutrophils to the tumour site. TM-28 expresses the human IL-8 cDNA under a tetracycline regulatable promoter, as well as neomycin and hygromycin resistance for selection purposes.

2.1.3 Response of Mutatect cells to mutations induced by irradiation

In order to assess the ability of the Mutatect cell lines to detect loss of hprt gene function with high sensitivity, the mutation frequency in response to ^{60}Co γ-radiation of the various cell lines was compared (Wilkinson et al., 1995). Radiation is a clastogenic agent with the ability to cause multi-locus lesions by the introduction, directly or indirectly, of double-strand breaks. MC-TGS17-51 and MN-11 were anticipated to be more sensitive to induction of 6-TG^R mutants when compared to the parental MC1A-C1 cells since the parental cells appeared to have two or more functional hprt genes. Thus, in order for a mutant to be scored in the parental cells, all of the hprt genes must be inactivated. MC-TGS17-51 and MN-11 showed steep dose dependent increases in the number of 6-TG^R colonies. This was in contrast to MC1A-C1, which produced virtually no mutant colonies over the dose range studied in several independent experiments. Cytotoxicity induced by radiation was similar for the three cell lines. At a radiation dose of 5 Gray (Gy), the induction of 6-TG^R colonies in MC-TGS17-51 and MN-11 was estimated to be ~1000 fold higher than in the parental cells.

This evidence supports the hypothesis that multiple hprt genes exist in the Mutatect cell lines and shows that MN-11 is able to detect mutations with a sensitivity within the range reported for other heterozygous marker genes (Schwartz et al., 1991).

2.1.4 Karyotype analysis of Mutatect cells

In order to determine the number of possible hprt genes in the Mutatect tumour cells, metaphase spreads of MC1A-C1, MC-TGR17, and MC-TGS17-51 were hybridized to biotinylated X-chromosome specific composite DNA probes (Breneman et al., 1995). The hybridized probe was detected using avidin-FITC, and showed that all Mutatect cell lines had less than four X-chromosomes. On average, ~3 X-chromosomes were detected in addition to several other regions elsewhere in the genome, which showed interstitial and centromeric X-specific sequences. Thus, since the hprt gene is normally X-linked, it appears that multiple copies are present in Mutatect cells.

2.1.5 Specific objectives

The possible presence of multiple hprt marker genes in Mutatect cells has direct implications on the sensitivity of this system to detect large-scale mutational events. Therefore, the initial objectives of my project are:

a) To determine if Mutatect cell lines are indeed heterozygous at the hprt locus by examining hprt cDNA for the presence of multiple copies.

b) To identify the mutation(s) which is/are responsible for the hprt$^-$ phenotype of MC-TGR17 so that these mutations can be excluded from future analysis of the wild type hprt marker gene.

2.2 Materials and Methods

2.2.1 Materials

A list of all reagents and suppliers is found in Appendix I.

2.2.2 Cell culture conditions

Mutatect fibrosarcoma cell lines were cultured in 10 cm tissue culture dishes (Falcon) with Dulbecco's modified Eagle medium (DMEM) plus 10% fetal calf serum (FCS) at 37°C and 5% carbon dioxide. Cells were sub-cultured by trypsinization approximately every 48 hr in order to maintain an exponential phase of growth. Stock cultures were frozen in liquid nitrogen at 1 x 10^6 cells/ml freezing medium (DMEM plus 20% FCS and 10% dimethyl sulfoxide).

2.2.3 Isolation of RNA from Mutatect cells

High molecular weight RNA (rRNA and mRNA) was extracted from MC1A-C1, MC-TGR17, MC-TGS17-51, and MN-11 cells as previously described (Birnboim, 1993). In brief, a monolayer of ~5 x 10^6 cells were lysed on ice in the presence of 1% sodium dodecylsulfate (SDS) and 1 M urea in order to inhibit ribonucleases. Chromosomal DNA was sheared by sonication, and protein was degraded by proteinase K digestion followed by two phenol/chloroform extractions. High molecular weight RNA was selectively precipitated using 3 M lithium chloride/40% ethanol. In order to lower the salt concentration, the RNA was dissolved and reprecipitated twice with 2 M sodium acetate and ethanol. The final pellet, containing purified RNA, was dissolved in 50 µl of CCS buffer (1

mM sodium citrate, pH 6.8, 1 mM 1,2-cyclohexanediaminetetraacetic acid (CDTA), 0.1% SDS) and stored at -20°C. The RNA concentration was determined by measuring the absorbance at λ=263 nm using a Perkin Elmer Lambda 14 UV/VIS spectrometer. To assess the integrity of the ribosomal RNA and to identify the presence of any significant amount of contaminating chromosomal DNA, 3 μg aliquots of each RNA sample were analyzed by electrophoresis through a 1.5% agarose gel followed by staining with 1 μg/ml ethidium bromide.

2.2.4 Reverse Transcriptase-Polymerase Chain Reaction analysis of hprt mRNA from Mutatect cells

To characterize the hprt genotype of the Mutatect cells, hprt cDNA was examined by reverse transcriptase-polymerase chain reaction (RT-PCR). Briefly, high molecular weight mRNA was transcribed into first-strand cDNA that was then amplified by PCR using hprt specific primers.

3 μg of RNA was precipitated from the CCS buffer by adding 0.1 vol 3 M sodium acetate, pH 5.6, and 2 vol cold ethanol. RNA was allowed to precipitate at -20°C for at least 30 min, then centrifuged at 13, 200 rpm (14, 500xg) for 5 min at room temperature. The supernatant was discarded and the RNA pellet was washed with cold 70% ethanol and centrifuged as above. The final pellet was resuspended in 10.4 μl of sterile H_2O pre-treated with diethyl pyrocarbonate (DEPC). 30 pmol of oligo $(dT)_{12\text{-}18}$ primer was added to the RNA, incubated at 65°C for 5 min and quenched on ice. 5X concentrated first strand buffer (250 mM Tris-HCl, pH 8.3, 375 mM KCl, 15 mM $MgCl_2$; GIBCO BRL), 0.5 mM dNTPs,

10 mM dithiothreitol (DTT), 200 U SuperScript reverse transcriptase (GIBCO BRL), and 20 U RNasin ribonuclease inhibitor (Promega) were added to give a final reaction volume of 20μl. The samples were incubated at 37°C for 1 hr and at 50°C for an additional 30 min. Negative controls were (I) reactions without reverse transcriptase enzyme (to demonstrate the absence of chromosomal DNA) and (ii) reactions which omitted the cDNA template. A 2 μl aliquot of the reverse transcription reaction was used as template for PCR amplification of hprt cDNA. PCR was carried out in sterile 0.6 ml thin-walled tubes and a total volume of 25 μl. The PCR was assembled on ice and consisted of 2 mM $MgCl_2$, 0.4 mM dNTPs, PCR buffer (20 mM Tris-HCl, pH 8.5, 50 mM KCl, 0.05% Tween 20), 10 pmol each of primers #55 and #151 (see Appendix II), and 2 U AmpliTaq DNA polymerase (Perkin Elmer). A drop of silicone oil was overlayed on each sample to prevent evaporation. The PCR tubes were placed in a pre-heated MJ Research Programmable Thermal Controller. The following cycle parameters were used: 95°C for 4 min followed by 30 cycles of 95°C for 1 min, 56°C for 1 min, and 72°C for 1 min. The final 72°C incubation was extended to 7 min. RT-PCR products were treated with ribonuclease A at a final concentration of 1 ng/μl for 10 min at 37°C to digest the rRNA in the reactions. RT-PCR products were examined by electrophoresis through a 1.5% agarose gel in TAC (40 mM Tris-HCl, pH 7.95, 20 mM sodium acetate, 1 mM CDTA) buffer, stained with 1 μg/ml ethidium bromide, and visualized under ultraviolet (UV) light.

2.2.5 Cloning of RT-PCR products into pCR2.1

Since multiple forms of hprt cDNA were expected, they were cloned in order to sequence individual cDNAs. The RT-PCR products from MC-TGR17 and MC-TGS17-51 were cloned directly using Invitrogen's pCR2.1 TA cloning kit. The pCR2.1 linear vector has single 3'-deoxythymidine residues at each end of the cloning site, which facilitates direct ligation with PCR products amplified using Taq polymerase (Figure 2-3). Taq polymerase has a non-template dependent activity, which adds a single deoxyadenosine to the 3' ends of the amplified DNA. Thus, the deoxyadenosine ends of the PCR products will bind to the deoxythymidine ends of the vector and facilitate ligation.

The RT-PCR products and the pCR2.1 vector were ligated together in a 1:1 molar ratio. In order to estimate the concentration of the cDNA product from the RT-PCR reactions, an ethidium bromide assay was used. A standard curve was constructed by mixing 4 μl of a 1 μg/ml solution of ethidium bromide with 4 μl of various concentrations of HL-60 DNA ranging from 0-20 ng/μl. The 8 μl dots were placed on an Ultra Violet Products White/UV Transilluminator lined with plastic wrap and photographed under UV light. The RT-PCR products were treated similarly, and their intensities were compared to those of the standards in order to estimate their DNA concentration.

The ligation reactions were assembled in sterile 0.6 ml tubes. Each reaction contained 50 ng (20 fmoles) of pCR2.1 plasmid DNA, ~11 ng of cDNA, 1 μl of 10X ligation buffer (60 mM Tris-HCl, pH7.5, 60 mM $MgCl_2$, 50 mM NaCl, 1mg/ml bovine serum albumin, 70 mM β-mercaptoethanol, 1 mM ATP, 20 mM

Figure 2-3. A schematic map of the pCR2.1 TA cloning vector.

A single-step cloning strategy allowed direct insertion of an RT-PCR product into the pCR2.1 vector by ligation of the cDNA to the 3' deoxythymidine overhang residues. The vector sequence includes an ampicillin and a kanamycin resistance gene for selection, the lacZα gene for blue-white colony screening, and ColE1 and F1 origins of replication. The multiple cloning site, within the lacZα gene, is flanked by M13 forward and reverse primer sequences which were employed for sequencing of the cDNA insert.

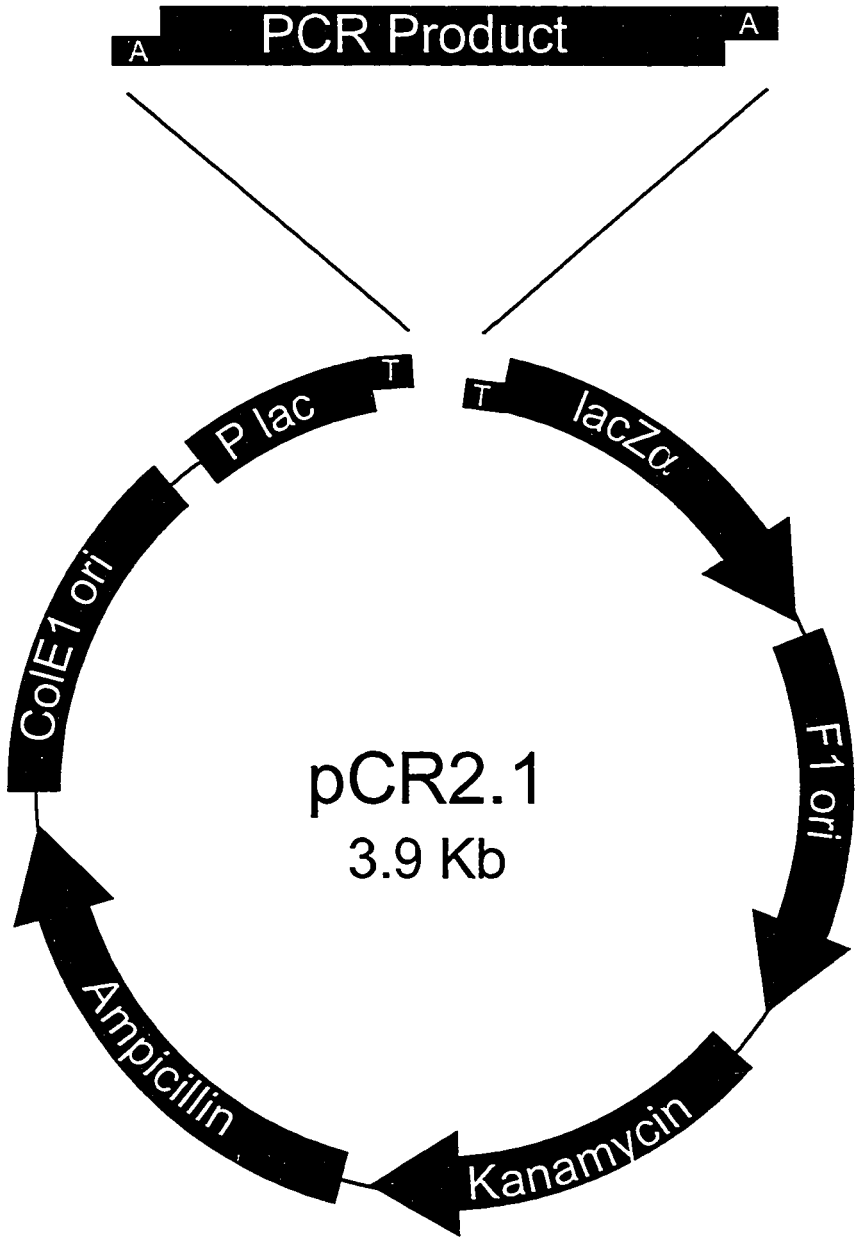
PCR Product
A
A
T
T
P lac
lacZα
ColE1 ori
F1 ori
pCR2.1
3.9 Kb
Ampicillin
Kanamycin

DTT, 10mM spermidine; Invitrogen) and 4 Weiss units of T4 DNA ligase (Invitrogen) in a total volume of 10 μl. The ligations were carried out at 14°C for 18 hrs and subsequently transformed into INVαF' One Shot competent cells (Invitrogen). 2 μl of 0.5 M β-mercaptoethanol and 2 μl of each ligation reaction were added to a vial containing 50 μl of INVαF' cells and mixed gently by stirring with a pipette tip. The vial was held on ice for 30 min, heat shocked for 30 sec in a 42°C waterbath, and returned to ice for an additional 2 min. 250 μl of SOC medium (2% tryptone, 0.5% yeast extract, 10 mM NaCl, 2.5 mM KCl, 10 mM $MgCl_2$, 20 mM glucose) was added to each vial and they were placed horizontally in a 37°C shaking incubator for 1 hr at 225 rpm. 50 μl of each ligation was spread on LB agar (1% tryptone, 0.5% yeast extract, 1% NaCl) plates containing 50 μg/ml ampicillin and 1.6 mg of 5-bromo-4-chloro-3-indolyl-β-D-galactoside (X-Gal). Once the liquid was absorbed, the plates were inverted and incubated at 37°C overnight.

2.2.6 Isolation of plasmid DNA from ampicillin resistant colonies

White colonies were selected randomly for plasmid DNA isolation using a modified alkyline lysis/polyethyleneglycol (PEG) precipitation method. All centrifugation steps in the following protocol were performed at 13,200 rpm in an International Equipment Company (IEC) Micromax microcentrifuge unless otherwise stated. Bacterial cultures were grown in 4 ml of terrific broth (1.2% tryptone, 2.4% yeast extract, 0.4% glycerol, 17 mM KH_2PO_4, 72 mM K_2HPO_4) containing 50 μg/ml ampicillin which was incubated overnight at 37°C and 225

rpm in a shaking incubator. 3 ml of each bacterial culture was pelleted in a 1.5 ml polypropylene microtube by 2 tandem spins of 1.5 ml aliquots for 1 min. After removing the supernatants by aspiration, the bacterial pellets were suspended in 200 µl of GTC buffer (100 mM glucose, 25 mM Tris-HCl, pH 8.0, 10 mM CDTA) containing 1 mg/ml lysozyme. Following an incubation period of 10 min at room temperature, 300 µl of freshly prepared 0.15N NaOH/1% SDS was added to each tube and mixed by inversion. A second 10 min incubation at room temperature was followed by addition of 300 µl of 3 M potassium acetate/1.8 M formic acid. The tubes were mixed by inversion and held on ice for 15 min. Cellular debris was removed by spinning for 10 min. The supernatant was transferred to a clean 1.5 ml microtube and ribonuclease A was added to a final concentration of 20 µg/ml. The tubes were incubated at 37°C for 20 min following which the samples were extracted twice with 400 µl of chloroform. After each extraction the tubes were mixed by hand and centrifuged for 1 min to separate the phases. The aqueous phase was removed to a clean 1.5 ml tube where the DNA was precipitated with an equal volume of isopropanol. The DNA was pelleted by centrifugation for 10 min. The DNA pellets were washed with 500 µl of 70% ethanol, dried under vacuum for 3 min, and dissolved in 32 µl of ddH_2O. Plasmid DNA was selectively precipitated by adding 8 µl of 4 M NaCl and 40 µl of sterile 13% PEG8000. After thorough mixing, the samples were incubated for 20 min on ice and then centrifuged for 15 min at 4°C and 14,000 rpm (19,800xg) in an Eppendorf 5417R centrifuge. After removing the supernatants, the pellets were dried under vacuum for 3 min and dissolved in 20

μl of H_2O. The plasmid DNA concentration was determined by reading the absorbance at λ=260 nm in a Perkin Elmer Lambda 14 UV/VIS spectrometer.

2.2.7 Screening of plasmid DNA by restriction digest

To identify which plasmids contained an hprt cDNA insert, the plasmid DNA was digested with EcoRI restriction enzyme. pCR2.1 contains an EcoRI recognition sequence on either side of the cloning site; therefore, those plasmids containing an insert will yield two fragments: one fragment of 3.9 kb corresponding to the vector sequence, and one fragment corresponding to the size of the cloned cDNA. 300 ng of plasmid DNA was combined with 2 μl of 10x React 3 buffer (500 mM Tris-HCl, pH 8.0, 100 mM $MgCl_2$, 1 M NaCl; Gibco), 5 U of EcoRI (Gibco), and H_2O to a total volume of 20 μl. The reaction was incubated at 37°C for 2 hr then stopped by adding 0.5 μl of 0.5 M CDTA. The restriction fragments were separated by electrophoresis through a 1.5% agarose gel, stained with 1 μg/ml ethidium bromide, and visualized under UV light.

2.2.8 Sequencing of cloned hprt cDNA

Those plasmids identified as containing a cDNA insert were further analyzed by sequencing. 500 ng of recombinant pCR2.1 plasmid DNA was sequenced using M13 forward and reverse primers that flanked the cloning site. Sequencing was performed using the dideoxy chain termination method (Sanger et al., 1977) at the University of Ottawa Biotechnology Research Institute, Ottawa, Canada.

2.2.9 High fidelity RT-PCR analysis

In order to minimize the number of nucleotide misincorporations that occur during the RT-PCR, a high fidelity polymerase (Vent DNA polymerase; New England Biolabs) was used. The RT reaction was carried out as described in section 2.2.3. 2 μl of the RT reaction provided the cDNA template for the PCR, which also included Thermopol buffer (10 mM KCl, 19 mM $(NH_4)_2SO_4$, 20 mM Tris-HCl, pH 8.8, 2 mM Mg_2SO_4, 0.1% Triton X-100; New England Biolabs), 0.4 mM dNTPs, 10 pmol each of primers #55 and 151, and 0.5 U of Vent DNA polymerase. The reactions were assembled in a total volume of 25 μl using 0.6 ml thin walled tubes and were placed in an Eppendorf Mastercycler Gradient thermocycler. The following parameters were used: 95°C for 3.5 min, followed by 30 cycles of 95°C for 1 min, 63°C for 1 min, 72°C for 1 min, and a final extension at 72°C for 5 min. Since the 3'-5' exonuclease activity of Vent polymerase produces blunt-ended PCR products, 2 U of AmpliTaq DNA polymerase were added to each reaction to incorporate deoxyadenosine residues onto the 3' ends. This was incubated at 72°C for 10 min, and then extracted with 40 μl of phenol/chloroform. After centrifuging for 2 min at 13,200 rpm (14,500 xg) in an IEC Micromax microcentrifuge, the aqueous phase was transferred to a new tube and mixed with 4 μl of 3 M sodium acetate and 90 μl of cold ethanol. The precipitated DNA was pelleted by centrifugation, as above, for 5 min. The pellets were washed with 70% ethanol and dissolved in 40 μl H_2O. The high fidelity RT-PCR products were cloned and sequenced in the same manner as described in sections 2.2.4-2.2.9.

2.3 Results

2.3.1 Multiple hprt cDNAs of the same size may be expressed by Mutatect cell lines

Previous experiments utilizing fluorescent *in situ* hybridization (FISH) of X-chromosome centromeric probes to MN-11 metaphase spreads have shown the presence of 3 X-chromosomes (Wilkinson et al., 1995). Presumably, due to an early non-disjunction event in the parental cells, the Mutatect cell lines maintain 3 X-chromosomes despite being isolated from a male mouse. Since the hprt gene resides on the X-chromosome, this evidence suggests that these cells contain 3 hprt genes. In order to address how many hprt genes were functional, we attempted to characterize the hprt genotype of the Mutatect cell lines by examining hprt cDNA using RT-PCR. Four cell lines from the Mutatect derivation pathway (Figure 2-2) were used: (i) MC1A-C1, the parental tumour cell line, (ii) MC-TGR17, which is 6-TG resistant (i.e. $hprt^-$ phenotype), (iii) MC-TGS17-51 which is a spontaneous revertant to HAT resistance (i.e. $hprt^+$ phenotype), and (iv) MN-11 which expresses the neomycin resistance gene for selection purposes. It was expected that all of the cell lines examined would express a full-length hprt cDNA, of either wild type, or a mutated version containing one or more point mutations. Since one of the hprt mutations sustained in MC-TGR17 was able to spontaneously revert back to wild type in MC-TGS17-51, it is probable that this was a small mutation, such as a base pair (bp) transition or transversion. Alternatively, it is possible that MC-TGS17-51 sustained a second mutation that was able to counteract the effects of the initial mutation and allow

for expression of a functional hprt protein. In either case, the size of the hprt mRNA is expected to remain indistinguishable from the wild type sequence. It was unknown whether the remaining two hprt genes, which presumably remained mutated in MC-TGS17-51 and MN-11, are able to express hprt mRNA. As expected, RT-PCR of RNA isolated from all of the Mutatect cell lines produced an 872 bp fragment, corresponding to the entire hprt coding region amplified by the primers used (Figure 2-4). Faint bands were also present at ~750 and 600 bp, but it is unknown whether these fragments contain hprt cDNA or a non-specific RT-PCR product. Therefore, if multiple hprt mRNAs are expressed, then the predominant message appears to be full-length.

2.3.2 Sequencing reveals hprt mutations that are a result of Taq DNA polymerase misincorporations

In order to determine the number of different hprt mRNAs that are expressed in Mutatect cells and to identify the mutations that cause MC-TGR17 to be 6-TG resistant, the RT-PCR products of MC-TGR17 and MC-TGS17-51 were cloned and sequenced. It was expected that MC-TGR17 would produce up to 3 different mutant forms of hprt mRNA, while in MC-TGS17-51 we anticipated that one of these mutated mRNAs would acquire a second mutation, or revert back to the wild type sequence. From the initial RT-PCR reactions (reaction A), a total of 9 clones from MC-TGR17 and 8 clones from MC-TGS17-51 were sequenced (Table 2-1). Several clones contained unique mutations within the hprt cDNA that were not found in any other clones. A total of 9 different mutant hprt cDNAs were identified suggesting that these mutations were likely an artifact

Figure 2-4. RT-PCR analysis of hprt cDNA from Mutatect cell lines.

First-strand cDNA was synthesized from high molecular weight RNA isolated from MC1A-C1, MC-TGR17, MC-TGS17-51, and MN-11. Hprt cDNA was then amplified using primers that flanked the entire hprt coding region. These primers are expected to amplify a fragment of 872 bp.

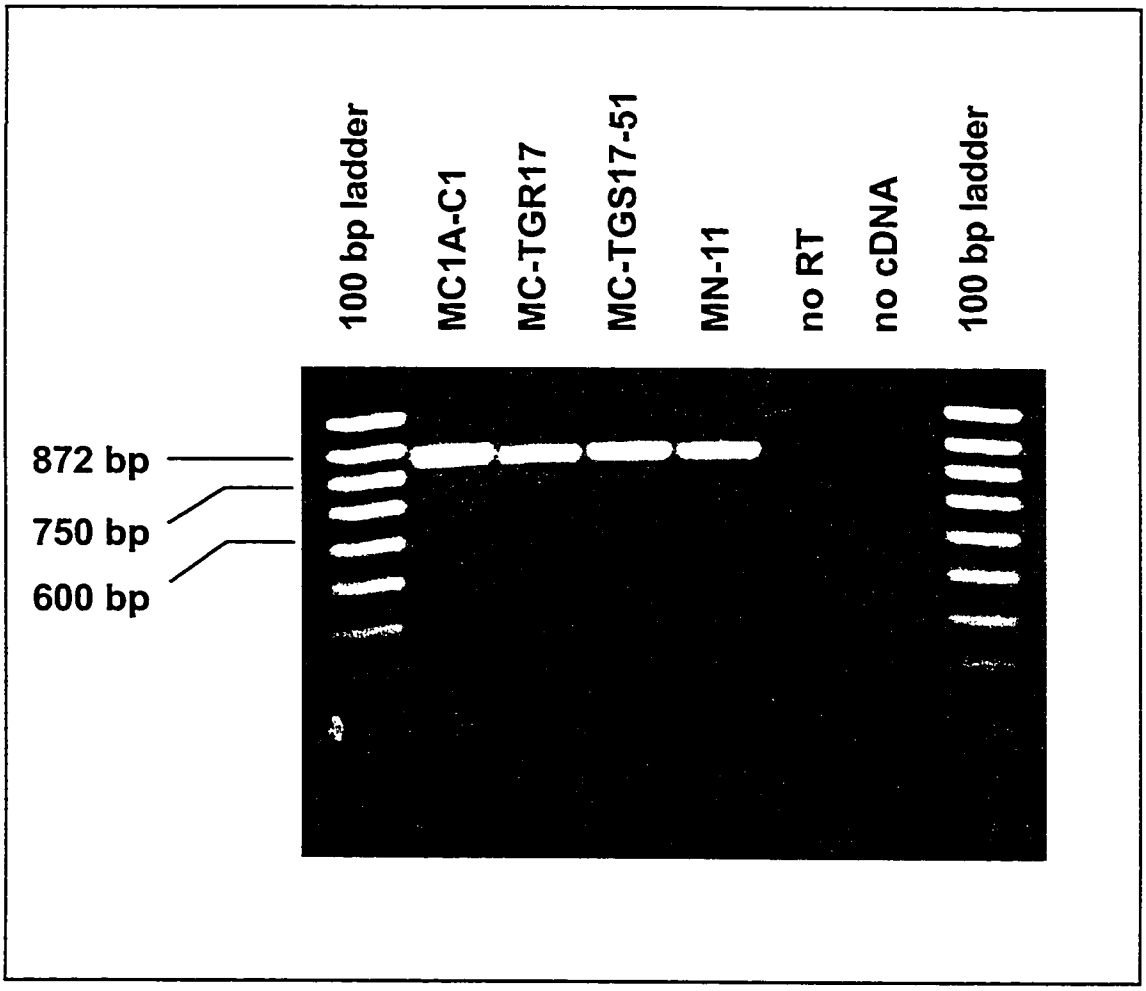
100 bp ladder
MC1A-C1
MC-TGR17
MC-TGS17-51
MN-11
no RT
no cDNA
100 bp ladder
872 bp
750 bp
600 bp

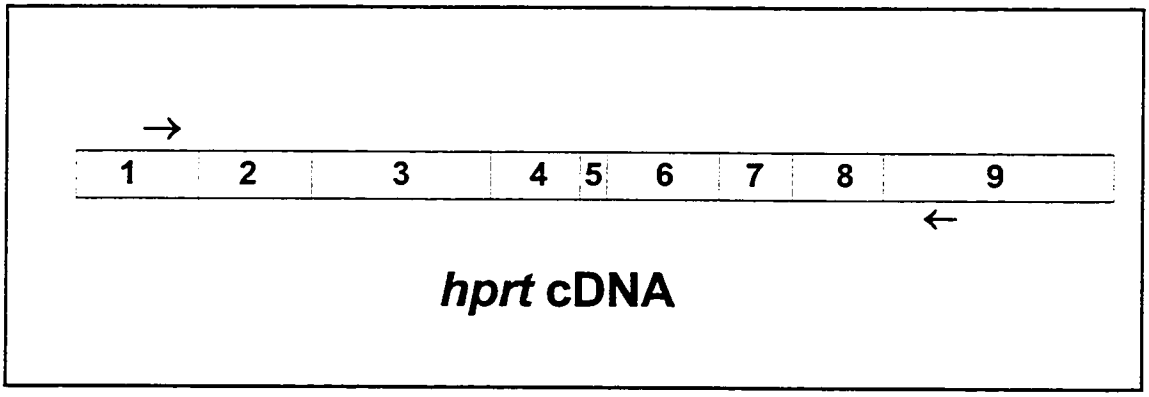
1
2
3
4
5
6
7
8
9
hprt cDNA

of the RT-PCR. In order to test this hypothesis, the RT-PCR was repeated (reaction B) using either Taq DNA polymerase, or Vent, a high fidelity polymerase, in the PCR reaction. Upon sequencing of these products, considerably fewer mutations were found (Table 2-1). Genuine mutations were confirmed by identifying at least two identical cDNA clones generated from independent RT-PCR reactions. The presence of two mutant hprt cDNAs from MC-TGR17 was confirmed by this method. The mRNA precursors to these cDNAs were designated mRNA-B (a single guanine deletion in exon 3) and mRNA-C (a deletion of exons 2 and 3) (Figure 2-5). Both of these mRNAs are maintained in MC-TGS17-51, and an additional wild type mRNA (mRNA-A) is expressed as well.

Table 2-1. Mutations identified in hprt cDNA clones by sequencing.

Hprt cDNA generated from MC-TGR17 and MC-TGS17-51 was cloned and sequenced using M13 forward and reverse primers. cDNA in reactions A and B was generated using Taq polymerase; cDNA in reaction B* was generated using Vent polymerase, a high fidelity enzyme with proofreading activity. The positions of the identified mutations are numbered according to the mouse hprt cDNA sequence published in genbank (J00423) with position 1 falling 88 nucleotides upstream of the translation start site. Highlighted sections indicate identical cDNAs generated from independent RT-PCR reations. Abbreviatons: Δ=deletion, w/t=wild type sequence, X→Y=base pair change.

MC-TGR17:Reaction A			MC-TGR17: Reaction B		
Number of clones sequenced	Position	Mutation	Number of clones sequenced	Position	Mutation
4	299	ΔG	1	299	ΔG
1	299 397 464 544	ΔG A→G C→T A→G	1	299 695 714	ΔG A→G T→C
1	267 299 610	T→C ΔG T→C	1	299 668	ΔG A→G
1	151 299	T→C ΔG			
2	116-406	Δexons 2,3			
MC-TGS17-51: Reaction A			MC-TGS17-51: Reaction B *		
2	-	w/t	5	-	w/t
1	528 866	T→C A→G	1	182	T→A
1	83 436	C →A A→G			
1	724 820	G→A C→A			
1	299	ΔG	1	299	ΔG
1	116-406 835	Δexons 2,3 T→C	1	116-406	Δexons 2,3

Figure 2-5. Multiple hprt mRNA species are present in Mutatect cells

Multiple hprt gene products were identified by sequencing RT-PCR cDNA clones from two Mutatect cell lines. Two mutant forms of the message are found in MC-TGR-17, designated mRNA-B and mRNA-C. Black boxes indicate wild type sequence, and angled lines represent deletions. mRNA-B has a frameshift mutation caused by a single guanine deletion within exon 3, while mRNA-C has a deletion of exons 2 and 3. mRNA-B and mRNA-C continue to be expressed in MC-TGS17-51 along with the wild type hprt message, mRNA-A.

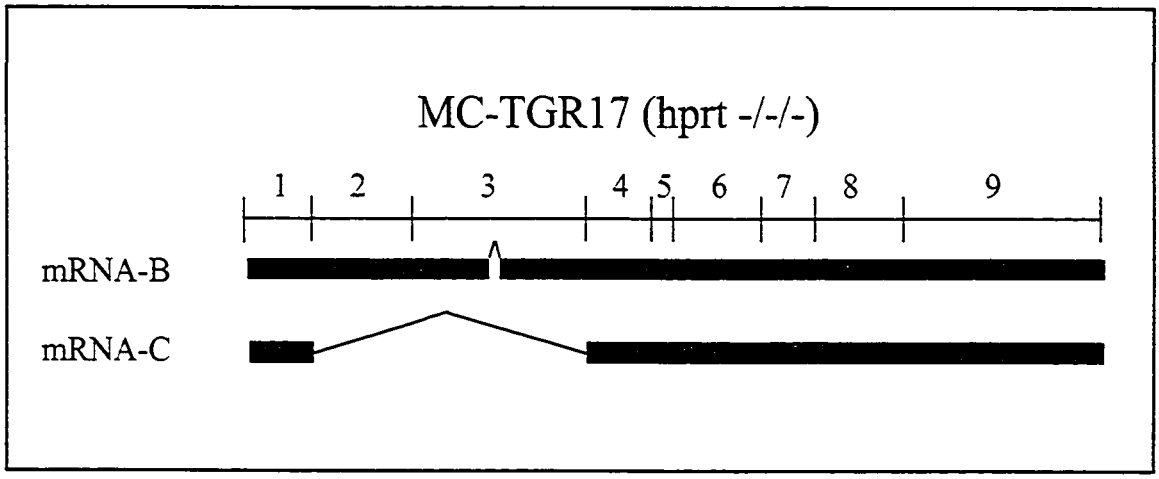
MC-TGR17 (hprt -/-/-)
1
2
3
4
5
6
7
8
9
mRNA-B
mRNA-C

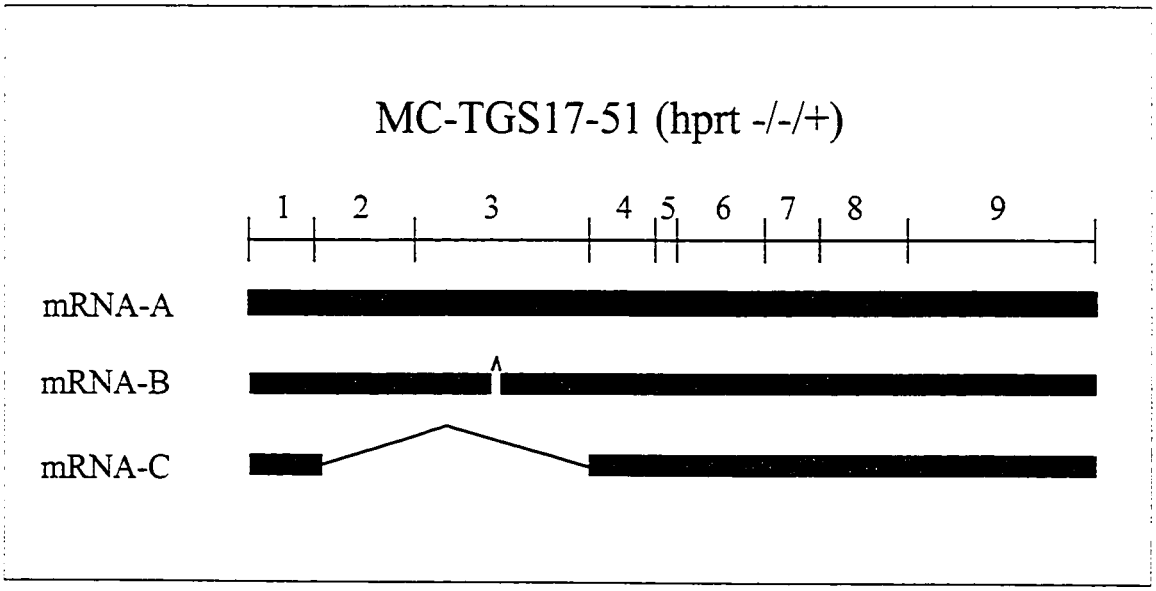
MC-TGS17-51 (hprt -/-/+)
1
2
3
4
5
6
7
8
9
mRNA-A
mRNA-B
mRNA-C

2.4 Discussion

Usually when multiple copies of the X-chromosome are found in mammalian cells (e.g. normal females, Kleinfelter's syndrome), all but one of the X-chromosomes are inactivated during development to allow for dosage compensation. However, in the case of the Mutatect cell lines, it appears that a mitotic non-disjunction event occuring during the transformation process has allowed for the expression of multiple X-chromosomes. While previous experiments provided indirect evidence of the presence of multiple (3) hprt genes, it was not until the hprt cDNA products were cloned and sequenced that direct evidence was generated to confirm that Mutatect cell lines are indeed heterozygous at this locus.

The predominant RT-PCR product, from the different Mutatect cell lines examined, corresponded to a full-length hprt cDNA (Figure 2-4). However, it was possible that multiple hprt cDNAs of a similar size were present in this band. Upon cloning and sequencing of individual hprt cDNAs, three different cDNAs were identified. During the development of the Mutatect cell lines, all three hprt genes appeared to be inactivated by treatment with MNU. MC-TGR17 ($hprt^-$ phenotype) was found to express only two mutant hprt mRNAs (mRNA-B and mRNA-C), which continue to be present in MC-TGS17-51 ($hprt^+$ phenotype). There was no evidence that a third mutated form of the gene was expressed, suggesting that the third copy of the gene contains a mutation either a) preventing it's expression (i.e., in the promoter region) or b) promoting instability of the message (i.e., in the 3' untranslated region). We propose that this third

mutant version of the hprt gene reverted back to wild type during the generation of MC-TGS17-51.

In addition to the full-length transcript, two minor RT-PCR products were visualized at 600 and 750 bp (Figure 2-4). Initially, it was unknown whether these minor products corresponded to hprt cDNAs expressed at a lower level, or were simply non-specific products of the RT-PCR. However, mRNA-C corresponds in size to the 600 bp RT-PCR product, suggesting that this minor constituent of the RT-PCR was an hprt-specific product. No 750 bp hprt cDNA clones were found which would explain the origin of the second minor RT-PCR product.

Numerous mutant hprt cDNA clones were generated from the RT-PCR reactions using Taq polymerase. These clones could not be confirmed in independent RT-PCR reactions, suggesting that these mutations were introduced by the polymerase during the PCR step. The fidelity of Taq polymerase has been reported to be 2.1×10^{-4} mutations per base duplication (Keohavong and Thilly, 1989) but is also dependent upon pH, magnesium ion concentration and dNTP concentration (Beltran et al., 2000). The fidelity of Vent polymerase, which contains a 3'→5' proofreading exonuclease activity, is reported to be 5-15 fold higher than that observed for Taq polymerase (Steinitz, 2000). This increase in fidelity is consistent with the decrease in mutant clones observed from the RT-PCR reactions generated using Vent polymerase (Table 2-1).

Interestingly, although MC-TGS17-51 expresses both mRNA-A and mRNA-B transcripts, the wild type message seems to be present at a higher level

than the mutant (ΔG) form (Table 2-1). The ratio of wild type to mutant (ΔG) clones is ~5:1 (assuming that the mutants containing base pair substitutions are due to Taq polymerase misincorporations and are in fact produced from wild type cDNA). Although not entirely representative of the cellular RNA distribution (due to the small number of clones sequenced) this ratio does suggest the possibilities that mRNA-B is more rapidly degraded or transcribed at a lower level than mRNA-A.

Although the mutations in mRNA-B and mRNA-C remain to be investigated at the genomic level, this work has generated sufficient information regarding the hprt locus so that the types of mutations induced in the wild type marker gene during *in vivo* or *in vitro* growth of Mutatect cells can be characterized. The results presented in this chapter will allow the characterization of the mutational spectrum induced by various treatments in future Mutatect experiments. This is beneficial to the Mutatect system since examining mutation frequency alone can be misleading. For example, if a mutation arises in a cell early during tumour growth, this cell has ample time to divide before the tumour is excised and the mutation frequency is calculated. Therefore a single mutational event may be unevenly represented in the final calculation. By characterizing the mutational spectrum, and eliminating those cells that have the same mutation at the same position, we can minimize this effect.

The Mutatect system is now a very powerful tool for examining the tumour environment and how factors present within this environment are contributing to

mutagenesis and to tumour progression. The effect of various physiologically relevant molecules, such as nitric oxide or reactive oxygen species, to the induction of mutations during solid tumour growth can be determined by this system. Moreover, whether the actions of antioxidants such as α-tocopherol are able to alleviate the production of these types of mutations and/or slow tumour progression can be investigated.

3. MOLECULAR CHARACTERIZATION OF HPRT MUTATIONS ARISING IN MUTATECT CELLS

3.1 Introduction

3.1.1 Mutational spectrums of mutagenic agents

Many studies have been conducted to determine the "spectrum" of genetic damage induced by various agents ranging from radiation to putative environmental toxins and carcinogens. Often, genotoxic agents produce a distinct mutational pattern, based upon the mechanism involved in initiation or repair of the damage. In order for such studies to be effective, it is imperative to know about the spontaneous spectrum of mutions that arise at any one marker locus.

3.1.2 Spectrum of spontaneous mutations arising In the hprt gene

In general, spontaneous mutations are thought to consist mainly of small point mutations and occasional small intragene deletions. Several studies have examined the *in vivo* spontaneous hprt mutation spectrum of T-lymphocytes isolated from peripheral blood of healthy people. Burkhart-Schultz et al. report 59% of hprt mutants contain base substitutions and 39% are comprised of deletion mutations (Burkhart-Schultz et al., 1996). Of these deletions, approximately equal proportions of frameshifts, small deletions of 3-200 bp, and large deletions were found. A study by Podlutsky et al. had similar findings with 76% base substitutions, 10% frameshifts, and 10% small deletions of 3-52 bp (Podlutsky et al., 1998). Both groups identified a number of "hotspots" within the

hprt coding sequence (i.e., positions at which the mutation frequency is significantly higher than would be expected based upon a Poisson distribution).

3.1.3 Spectrum of mutations induced by X rays at the hprt locus

In contrast to the spectrum of spontaneous mutations, the majority of radiation-induced mutations tend to be large-scale deletions. This can be attributed (directly or indirectly) to the production of double-strand breaks within DNA, which, if not properly rejoined, lead to the loss of large chromosome segments. Deletions accounted for 72% of the hprt mutants isolated after exposure of WTK-1 (a human lymphoblastoid cell line expressing mutant p53) to 2 Gy of X rays (Phillips et al., 1995). Approximately half of these mutants contained large deletions eliminating the entire hprt gene and several adjacent X-linked markers.

3.1.4 Spectrum of mutations associated with nitric oxide production

The spectrum of nitric oxide induced mutations resembles that of spontaneous mutants. RAW264.7 macrophages, stimulated to produce nitric oxide by interferon-γ and lipopolysaccharide, were found to contain mainly base substitutions and single exon deletions—mutations that did not differ significantly from those observed in spontaneous controls or cells treated with a NOS inhibitor (Zhuang et al., 1998). The only mutations that could be attributed solely to the action of NO were small deletions (<72bp) or insertions and multiple exon deletions. Similar results were obtained by the same group when they examined

TK6 cells and *Salmonella typhimurium* after exposure to NO (Zhuang et al., 2000). Thus, they have postulated that reactive species derived from NO may contribute to spontaneous mutagenesis.

It is important to note that both of these studies characterized the hprt mutations by sequencing of RT-PCR products. In their analyses, an RT-PCR product was obtained for only 41% and 60%, respectively, of the mutant clones examined. Thus, a large fraction of hprt mutants is missing from their investigation, which may represent a population containing large-scale deletions.

3.1.5 Mutation frequencies observed in Mutatect cell lines

The frequency of mutation observed in Mutatect cell lines is significantly elevated when they are grown *in vivo* as a subcutaneous tumour as compared to growth in culture. MN-11 cells exhibit a 3.4 fold increase in mutation frequency with *in vivo* growth {Wilkinson, 1995, 5504/id}, while TM-28 (which expresses IL-8 and attracts neutrophils to the tumour site) shows a 36-fold increase compared to *in vitro* controls {Sandhu, 2000, 6768/id}. Thus, we expect that a higher number of $hprt^-$ mutants collected from the TM-28 tumours will be a result of mutations induced by factors present within the tumour microenvironment as opposed to spontaneous events. Additional experiments conducted in our laboratory have increased the *in vivo* mutation frequency of MN-11 tumours by injecting the mice with glyceryl trinitrate (GTN) prior to tumour excision. This treatment does not influence the neutrophil composition of the tumours, but is

able to raise the mutation frequency ~7-fold, presumably as a result of the genotoxic actions of reactive nitrogen species {Sandhu, 2000, 6768/id}.

3.1.6 Strategy to identify large-scale deletions in Mutatect cells

The genotype characterization of Mutatect cells, presented in chapter 2, revealed that 3 different hprt messages are transcribed. Two of these mRNAs, mRNA-B and mRNA-C, contain mutations that lead to the production of a non-functional hprt protein. The remaining message, mRNA-A, is wild type and acts as the marker gene for the selection of hprt mutants in Mutatect cells. Thus, in order to characterize the types of mutations that arise in the functional hprt gene, a strategy must be developed to facilitate the differentiation between it and the remaining 2 genes, which are already mutated.

Due to the complexity of the hprt locus in Mutatect cells, we decided to focus on characterizing alterations in the mRNA of hprt mutants. mRNA-C can be readily distinguished from the other mRNAs on the basis of size, since it is missing a 291 bp section corresponding to exons 2 and 3. However, the difficulty lies in distinguishing mRNA-A from mRNA-B, which differ only by the presence or absence of a single guanine nucleotide within exon 3. It is also important to note that this nucleotide is located within a short polypurine tract of 6 guanines, further complicating the process of differentiating between the two messages.

A sequencing strategy was developed that could determine which mutants had lost expression of mRNA-A (possibly due to the presence of a large-scale deletion), and which mutants retained its expression but with a mutation within

the coding region (Figure 3-1). This strategy involves a combination of RT-PCR and manual sequencing over the region of the single guanine deletion (position 299) in mRNA-B. By using RT-PCR primers located in exons 2 and 3, mRNA-A and B can be selectively amplified into cDNA since this region is not present in mRNA-C. Sequencing of the RT-PCR products using ddGTP chain terminators will produce a different pattern of nucleotides depending on whether mRNA-A and B are expressed alone or in combination. If both mRNA-A and mRNA-B are expressed in a mutant clone, 6 guanines will be present at position 299 on the sequencing gel, and the sequence past this position will be offset by one nucleotide due to the frameshift mutation in mRNA-B. If only mRNA-B is expressed, 5 guanines will be present in this region, and the sequence will remain clean.

3.1.7 Specific objective

a) To develop a method for screening mutant hprt clones of Mutatect cells for the possible presence of large-scale deletion mutations.

Figure 3-1. Sequencing strategy developed to screen Mutatect hprt$^-$ mutants

The screening strategy involves amplifying hprt cDNA of exons 2 and 3, and sequencing these products in a single reaction using [α-^{33}P] ddGTP chain terminators. mRNA-C will not produce an RT-PCR product since the primer binding sites lie within the deleted region, depicted by a black box. By sequencing over the region of the single guanine deletion in mRNA-B, two groups of mutants will be distinguishable. Those mutants that have lost expression of mRNA-A will display 5 guanines in this region, while mutants that retain expression of mRNA-A will display 6 guanines. In the latter situation, the sequence past this region will be offset by one nucleotide due to the presence of mRNA-B.

1. RT-PCR

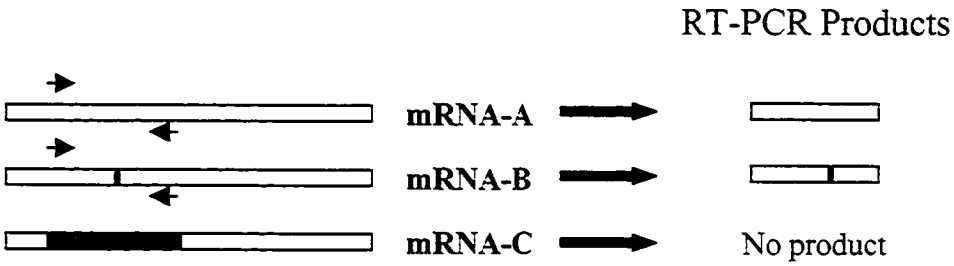

2. Sequencing of RT-PCR Products

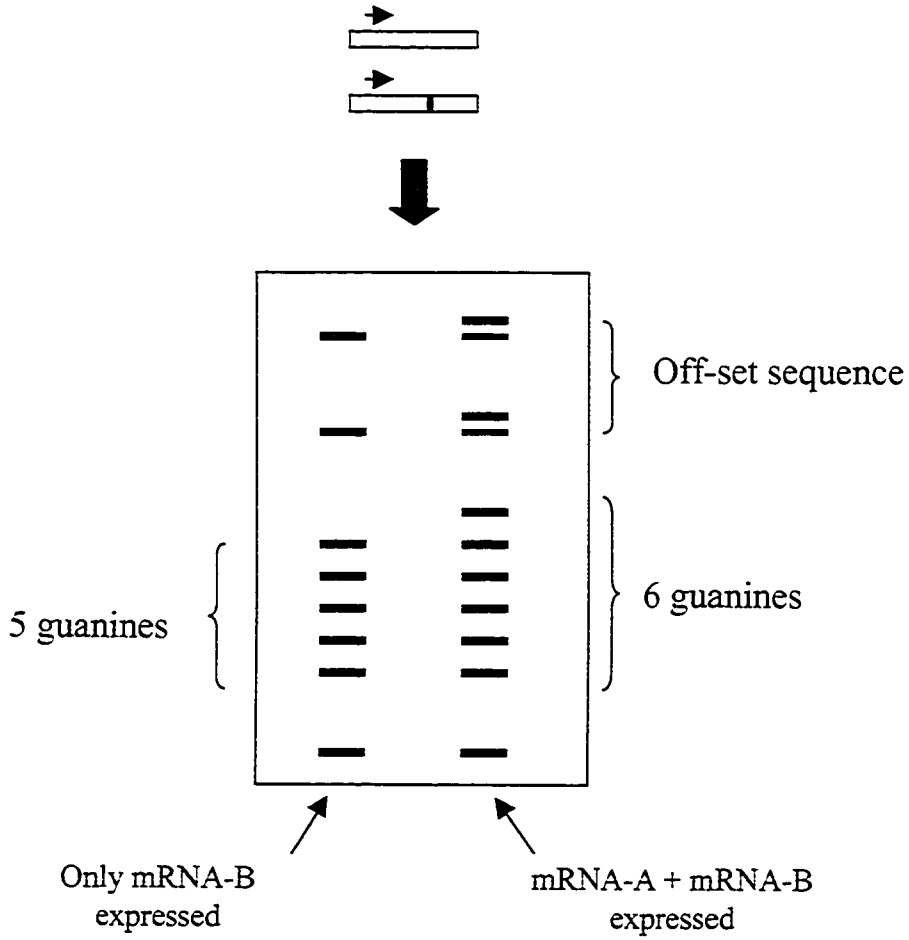

3.2 Materials and Methods

3.2.1 Materials

A list of all reagents and suppliers is found in Appendix I.

3.2.2 Cloning of hprt mutant colonies

Hprt mutant Mutatect cells were generated in a variety of experiments described in detail in the following sections. After the experimental treatment, cells were maintained in culture for 8 days, with subculturing by dilution in fresh medium as needed. This period allows for expression of a mutant hprt phenotype (i.e., for any remaining wild type hprt protein to be degraded and for new mutant protein to be synthesized). On day 9 post-treatment, cells were counted by hemocytometer using trypan blue exclusion as a measure of viability. 1×10^5 viable cells were plated per 10 cm tissue culture dish and were challenged with 6-TG medium (DMEM plus 10% FCS and 50 μM 6-TG) for 10 days to allow for mutant hprt colonies to form. Cells from individual colonies were picked with a pipet tip and transferred to separate wells of a 96-well plate. Hprt mutant clones were expanded in culture until adequate numbers were achieved for RNA extraction.

3.2.3 Cell irradiation

MN-11 cells were plated at 1×10^6 and 2×10^6 cells per 10 cm tissue culture dish in non-selection medium (DMEM plus 10% FCS). Cells were irradiated on ice with 3 or 5 Gy respectively using the X-ray source at the Ottawa

Regional Cancer Centre, Cancer Research Group. Beginning 24 hours after irradiation, cells were subcultured by dilution in fresh medium at a ratio of 1:4, every 2-3 days. In this way, cells were maintained in culture for a period of 8 days to allow for expression of a mutant hprt phenotype. On day 9 after irradiation, cells were challenged with 6-TG and individual colonies were cloned as described above.

3.2.4 Generation of *in vivo* hprt mutants using the Mutatect model

TM-28 Mutatect cells were cultured for 7 days in non-selection medium supplemented with HAT (1×10^{-4} M hypoxanthine, 4×10^{-7} M aminopterin, and 1.5×10^{-5} M thymidine) in order to eliminate any pre-existing $hprt^-$ mutants. Cells were then washed with sterile phosphate buffered saline (PBS) (140 mM NaCl, 2.7 mM KCl, 8 mM Na_2HPO_4, 1.5 mM KH_2PO_4, pH 7.4) and cultured in HT medium (non-selection medium plus 1×10^{-4} M hypoxanthine, and 1.5×10^{-5} M thymidine) for an additional 2 days to allow for complete aminopterin depletion. 5×10^5 viable cells, determined using a hemocytometer and trypan blue exclusion, were injected subcutaneously into the hind flank of C57Bl/6 female mice, 8-10 weeks of age (Charles River Laboratories). TM-28 cells were injected in 200 µl of sterile PBS containing 1 mg/ml tetracycline in order to repress their IL-8 expression while tumours became established. When tumours reached ~1 cm in diameter (approximately 2-3 weeks after tumour inoculation), the animals were euthanised by cervical dislocation and the tumours were excised. Tumours were cut into small pieces and mechanically homogenized using a 3 c.c. syringe

(without needle) to create a cell suspension. Tumour cells were allowed 2-4 days to establish culture in non-selection medium before 6-TG selection was applied.

3.2.5 *In vitro* spontaneously arising mutants

A portion of the HAT/HT selected TM-28 cells were maintained in culture for the duration of the *in vivo* mouse experiment, in order to generate a population of *in vitro* spontaneous hprt$^-$ mutants to act as a control. Cells were plated at 1 x 10^5 cells in 12 separate 10 cm tissue culture dishes in non-selection medium, and subcultured as needed by dilution in fresh medium for a period of 25 days. Each plate of TM-28 cells was challenged separately with 6-TG, and one hprt$^-$ mutant was isolated from each plate. This ensured that each mutant isolated arose from an independent mutagenic event.

3.2.6 *In vivo* glyceryl trinitrate induced mutants

Glyceryl trinitrate (GTN) induced mutants were generated from an in vivo experiment utilizing MN-11 cells. These cells were treated identically to the TM-28 cells described in section 3.2.3, with the exception that tetracycline was omitted during the tumour injection. 12 days post-injection of tumour cells, mice were given an intraperitoneal injection of GTN (5 mg/kg). A control group of animals was similarly injected with PBS. Two days after treatment, tumours were excised and established in culture as described in section 3.2.3. This experiment

was conducted by Dr. Jagdeep Sandhu, who kindly provided the GTN-induced mutants for molecular analysis.

3.2.7 RT-PCR of hprt mutant clones

Hprt$^-$ mutant clones, generated from the above experiments, were expanded in culture to achieve sufficient numbers for RNA extraction. High molecular weight RNA was extracted as described in section 2.2.2. The extracted mRNA was reverse transcribed into cDNA using the RT reaction described in section 2.2.3. 2 μl of the RT reaction provided the template DNA for the subsequent PCR using Clonetech's Advantage HF-2 kit. PCR reactions were assembled in sterile 0.2 ml thin-walled tubes and consisted of 2.5 μl each of 10X HF-2 PCR buffer and 10X HF-2 dNTP mix, 0.5 μl of 50X Advantage HF-2 polymerase mix, 10 pmoles each of primers #188 and #189 (Appendix II), and 15.5 μl of sterile H_2O. The reaction tubes were placed in a GeneAmp 9600 thermocycler (Perkin Elmer) and incubated as follows: 94°C for 3 min, 35 cycles of 94°C for 30 sec, 59°C for 30sec, and 72°C for 1 min, followed by a final extension at 72°C for 5 min. The reactions were treated with 4 μl of 5 ng/μl ribonuclease A at 37°C for 10 min to digest the remaining rRNA. RT-PCR products were examined by electrophoresis through a 1.5% agarose gel in TAC (40 mM Tris-HCl, pH 7.95, 20 mM sodium acetate, 1 mM CDTA) buffer, stained with 1 μg/ml ethidium bromide, and visualized under ultraviolet (UV) light.

3.2.8 Sequencing of RT-PCR products

The RT-PCR products were purified using Microcon filters (Amicon), in order to remove unincorporated nucleotides, primers, and to reduce the salt concentration prior to sequencing. 475 µl of sterile H_2O and the RT-PCR sample were added to the Microcon filter unit and centrifuged at 3, 000 rpm (1, 000 xg) for 15 min. The flow-through was discarded and the filter unit was inverted in a clean tube for recovery of the cDNA, which was accomplished by adding 20 µl of sterile H_2O to the inverted filter unit and centrifuging, as above, for 2 min.

1 µl of the purified RT-PCR products was sequenced using [α-^{33}P] labelled dideoxynucleotide (ddNTP) terminators and Amersham's ThermoSequenase Radiolabelled Terminator Cycle Sequencing kit. Sequencing reactions were assembled in 0.6 ml thin-walled tubes, each containing 2 µl of dNTP master mix, 0.5 µl of the appropriate [α-^{33}P] ddNTP (1500 Ci/mmol, 450µCi/ml), 0.5 µl of 10X reaction buffer (260 mM Tris-HCl, pH 9.5, and 65 mM $MgCl_2$), 0.5 pmol of primer #190 (Appendix II), 2 U of ThermoSequenase polymerase, and sterile H_2O to bring the total reaction volume to 7.5 µl. The tubes were placed in a pre-heated Eppendorf Mastercycler Gradient thermocycler. Thirty cycles of the following parameters were used: 95°C for 30 sec, 45°C for 30 sec, and 72°C for 1 min. 4 µl of stop solution (95% formamide, 20 mM EDTA, 0.05% bromophenol blue, 0.05% xylene cyanol) was added to each reaction prior to denaturation at 70°C for 10 min. Sequencing reactions were resolved on a 6% acrylamide/7 M urea gel using TBE buffer (89 mM Tris-HCl, 89 mM boric acid, 2 mM EDTA, pH 8.3). The gel was pre-run for 15 min prior to loading of samples. Electrophoresis was

carried out at 100 watts for approximately 2.5 hours, following which the gel was transferred to 3 MM Whatmann filter paper and dried under vacuum at 80°C for 1.5 hours. Autoradiography was performed by exposing the dried gel to Kodak X-Omat Blue XB-1 film for ~48 hours.

3.3 Results

3.3.1 Sequencing strategy is able to detect loss of hprt mRNA-A

In order to characterize the types of mutations that are generated during *in vivo* growth of Mutatect cells, a strategy was needed that would distinguish the three different hprt genes. We are interested in studying mutations that occur in the wild type marker gene (gene A); however, the presence of two other non-functional hprt genes (genes B and C) complicates this process. In particular, we are looking for the presence of large-scale deletion mutations. Therefore a strategy was designed to differentiate between mutations that affect the expression of mRNA-A (i.e., possibly large deletions) and those that do not (i.e., base substitutions within the coding region).

X-rays, at doses of 3 and 5 Gy, were used to induce mutations in Mutatect cells at the hprt locus. Since ionizing radiation has been well documented to cause large multi-locus deletions, these mutants provided a positive control to test the ability of the sequencing strategy to detect mutations that prevent the expression of hprt mRNA-A. It was expected that the majority of radiation-induced mutants would have lost the hprt marker gene due to a large-scale deletion at this location. A total of 15 independent X-ray induced $hprt^-$ mutants were examined. Sequencing of the RT-PCR products revealed that all 15 of the radiation-induced mutants contain 5 guanines at the region of interest (position 299 within exon 3), indicating that a single RT-PCR product from mRNA-B was present (Figure 3-2). MC-TGS17-51, the Mutatect cell line expressing all three

Figure 3-2. Screening of X-ray induced hprt mutants by sequencing of RT-PCR products

RD-3 and RD-5 hprt mutants were generated by irradiating MN-11 cells with 3 or 5 Gy of X-rays, respectively. Mutant hprt cDNA was amplified over exons 2 and 3 and sequenced using [α-^{33}P] ddGTP chain terminators. Each lane corresponds to an individual mutant clone. p1751-A, a plasmid containing wild type hprt cDNA, and MC-TGS17-51 were included as controls. MC-TGR17, which does not express mRNA-A, was sequenced using all four ddNTP terminators so that the region of interest could be easily identified.

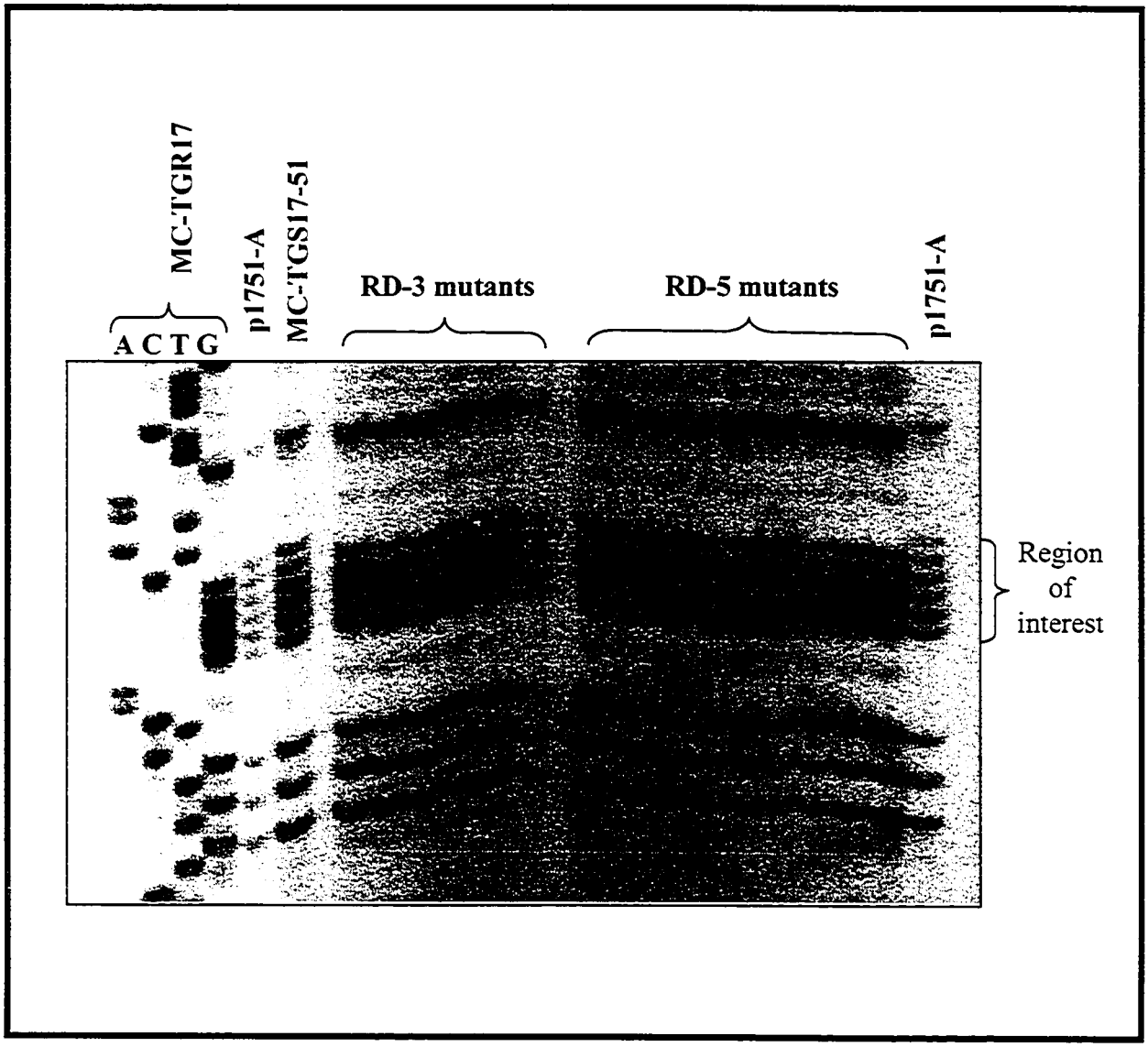
MC-TGR17
A C T G
p1751-A
MC-TGS17-51
RD-3 mutants
RD-5 mutants
p1751-A
Region
of
interest

hprt mRNAs, was included as a control. As expected, this cell line shows the presence of 6 guanines, in addition to faint bands visible in the downstream sequence that are offset by one nucleotide. Plasmid p1751-A, containing the wild type hprt cDNA, was included as a second control. It displays 6-guanines, and the downstream sequence remained clean, as expected. MC-TGR17, which expresses mRNA-B only, acts as another positive control and displays only 5 guanines in the region of interest. Therefore, the sequencing strategy used is capable of distinguishing between cells that express mRNA-A and/or mRNA-B, and can detect mutations that prevent expression of the former.

3.3.2 Analysis of *in vitro* spontaneous mutants

TM-28 cells were grown in culture for a period of 25 days, after which spontaneously arising 6-TG resistant colonies were cloned. It was expected that the majority of these mutants would retain expression of hprt mRNA-A, since we anticipated mostly base substitutions. However, upon sequencing of the RT-PCR products, all 11 mutants analyzed showed an identical pattern of 5 guanines, implying that the wild type sequence corresponding to this region was absent (Figure 3-3). The controls described above (section 3.3.1) were also included, and produced the same results as in figure 3-2. This indicates that, if the wild type sequence had been present in the spontaneous mutants, the sequencing method would have been sensitive enough to detect it (as was seen for MC-TGS17-51).

Figure 3-3. Screening of TM-28 spontaneous hprt mutants for the presence or absence of mRNA-A.

TM-28 spontaneous hprt mutants arising during *in vitro* culture or *in vivo* tumour growth were cloned. Mutant hprt cDNA was amplified over exons 2 and 3 and sequenced using [α-^{33}P] ddGTP chain terminators. Each lane corresponds to an individual mutant clone. p1751-A, a plasmid containing wild type hprt cDNA, and MC-TGS17-51 were included as controls. MC-TGR17, which does not express mRNA-A, was sequenced using all four ddNTP terminators so that the region of interest could be easily identified.

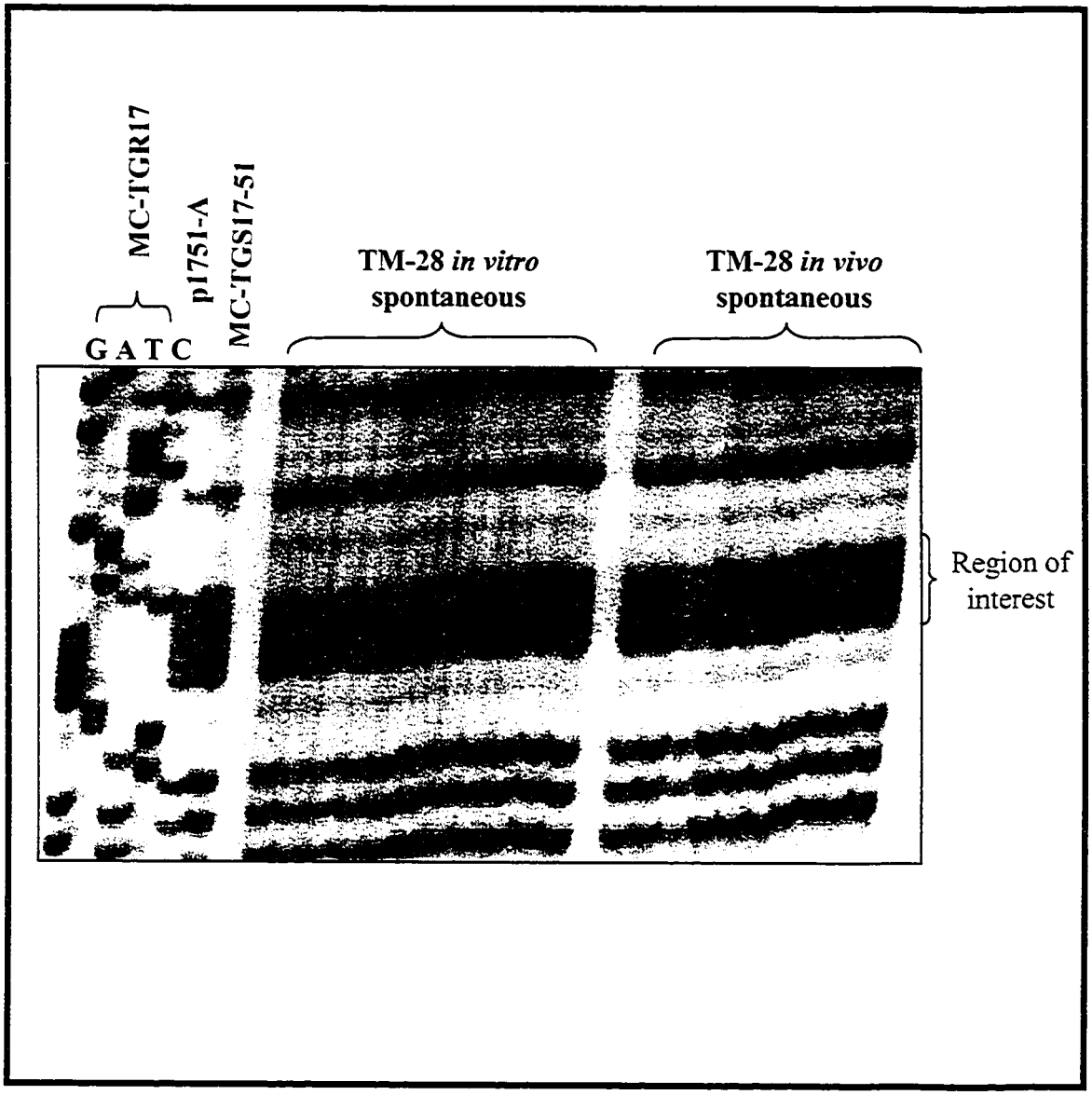
MC-TGR17
p1751-A
MC-TGS17-51
G A T C
TM-28 *in vitro* spontaneous
TM-28 *in vivo* spontaneous
Region of interest

3.3.3 *In vivo* mutants show a high frequency of possible hprt gene loss events

In vivo mutants were generated either spontaneously (TM-28) or by treatment with glyceryl trinitrate, a source of nitric oxide. A total of 3 GTN-induced mutants and 26 spontaneous mutants were examined (Figures 3-3 and 3-4). As for the previous figures, all mutants arising during *in vivo* tumour growth have 5 guanines at the region of interest in the hprt cDNA, while both positive and negative controls appear as expected. Although we expected to see some *in vivo* mutants that retained the 6-guanine sequence, we found that none of the mutants analyzed retained the wild type sequence in this region.

Figure 3-4. Screening of hprt mutants generated during in vivo tumour growth.

TM-28 hprt mutants arose spontaneously during in vivo growth, while MN-11 mutants were induced by GTN treatment. Mutant hprt cDNA was amplified over exons 2 and 3 and sequenced using [α-^{33}P] ddGTP chain terminators. Each lane corresponds to an individual mutant clone. p1751-A, a plasmid containing wild type hprt cDNA, and MC-TGS17-51 were included as controls. MC-TGR17, which does not express mRNA-A, was sequenced using all four ddNTP terminators so that the region of interest could be easily identified.

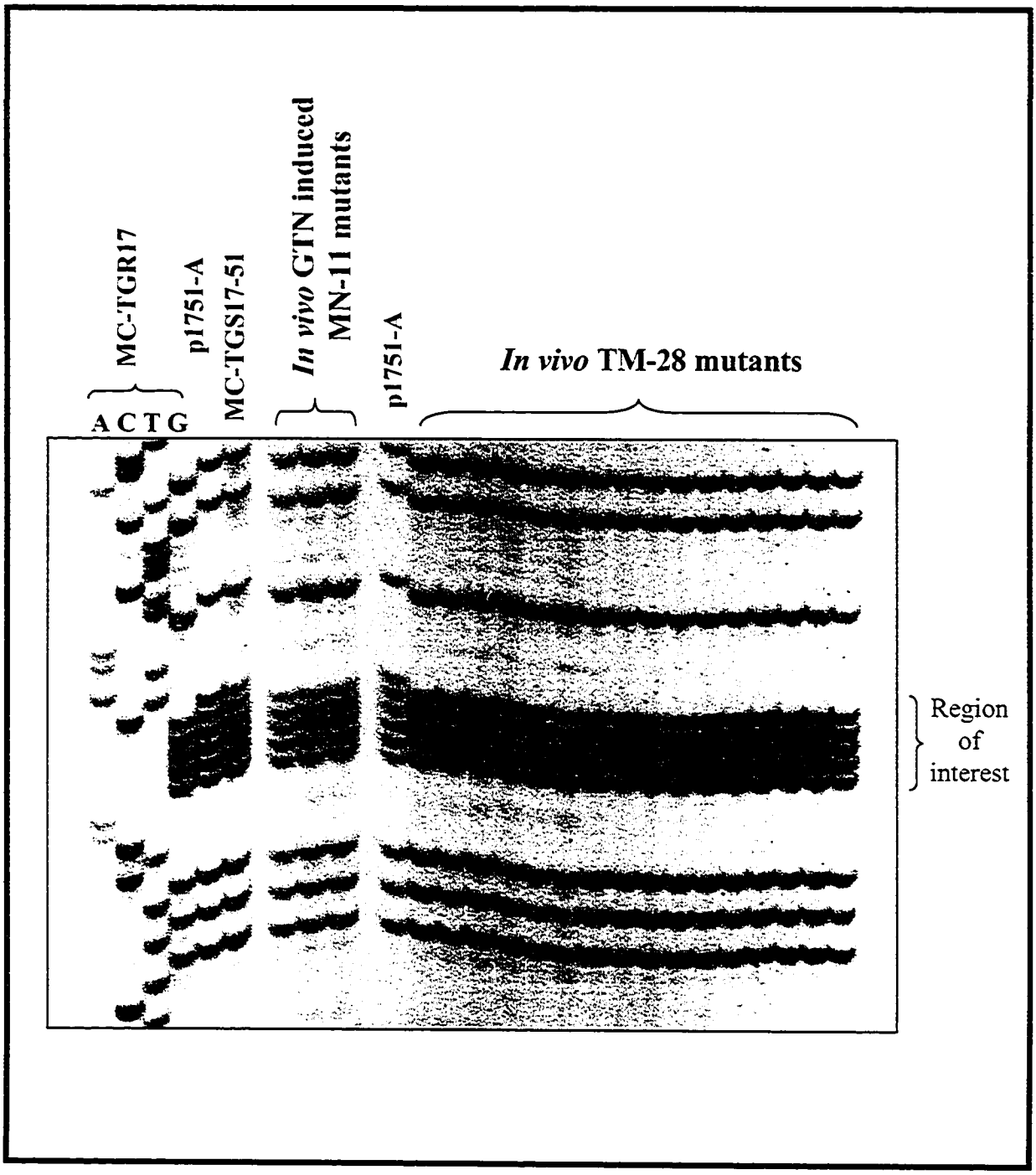
MC-TGR17
A C T G
p1751-A
MC-TGS17-51
In vivo GTN induced MN-11 mutants
p1751-A
In vivo TM-28 mutants
Region of interest

3.4 Discussion

Mutatect cells are known to be sensitive to the *in vitro* induction of mutations by ionizing radiation, radiomimetic drugs, and nitric oxide-donating drugs, as seen by an increase in mutant frequency at the hprt locus (Sandhu and Birnboim, 1997). The presumed heterozygous nature of the hprt gene was thought to account for the high frequency of mutations observed, by allowing Mutatect cells to tolerate large-scale deletions at this locus. The hprt genotype was confirmed to be heterozygous through results presented in chapter 2. Our focus then shifted to the molecular characterization of the mutations that were being induced in Mutatect cells, with emphasis on determining whether large-scale deletions were present.

Ideally, it would have been more informative to be able to study mutants at the DNA level; however, the presence of 3 hprt genes in these cell lines made traditional analysis via Southern blotting very difficult. Thus, the mutants were characterized at the mRNA level using a strategy combining RT-PCR and sequencing. While this strategy was an efficient means of screening many mutants for possible hprt gene loss, it does not definitively prove that gene loss has occurred. For example, there are several other types of mutations besides large deletions that could prevent expression of the hprt gene. These include small mutations within the promoter or 3'-untranslated region that may affect levels of gene expression or mRNA stability, respectively. Changes in DNA methylation patterns, which play a role in gene silencing, could also prevent transcription of mRNA-A. As well, any mutation within the RT-PCR primer

binding sites might prevent amplification of a cDNA product. Point mutations occurring in the splice acceptor or donor sites could also affect the production of cDNA during the RT-PCR if exon 2 or 3 were spliced out of the mRNA. Thus, as well as large-scale deletions, this screening method may also be detecting smaller mutations that affect either gene expression or the ability to produce an RT-PCR product.

The same nucleotide pattern was observed in all of the mutant clones examined, whether generated *in vitro* or *in vivo*, spontaneously or induced (Figures 3-2, 3-3, 3-4). This brings up the question of whether these are indeed independent mutants, or perhaps "siblings" arising from the same mutational event. For example, if a mutation is induced in a single cell early during tumour formation, this cell has the opportunity to undergo several divisions before the mutant cells can be cloned. Therefore, many of the hprt mutant clones collected from a single tumour may be generated from the same mutational event, and would display the same pattern upon molecular analysis. Careful attention was paid to this issue when selecting 6-TG resistant clones. Only one mutant was selected from each tissue culture dish from *in vitro* experiments, and similarly, only 1-2 mutants were cloned from each mouse tumour. Thus, each Mutatect clone that was screened was likely generated by a separate mutation.

It was surprising to find that none of the mutants retained a wild type sequence at position 299, considering the types of mutational spectrums that were previously reported (see sections 3.1.2-3.1.4) at the hprt locus. However, it is important to note that the hprt locus in all of these studies is hemizygous, and

therefore is biased against detecting large-scale deletions. The rate of mutation induction by radiation is 10-100X lower in hemizygous genes (Evans et al., 1986). Our findings are consistent with those reported at heterozygous loci in a variety of different cell lines. Studies using a heterozygous aprt gene, each in a different cell line, all show a high frequency of spontaneous gene deletion (>95% gene loss reported by Turker et al.), as well as frequent loss of adjacent markers suggestive of multi-locus deletions (Dewyse and Bradley, 1989). Evans found a similar trend in L5178Y mouse lymphoblasts, where the majority of spontaneous, X-ray, and ultraviolet (UV) radiation-induced mutants showed loss of the active allele at the heterozygous thymidine kinase locus (Evans, 1994). Therefore, it seems possible that many of the Mutatect mutants may, in fact, contain complete gene deletions at the hprt locus. Further characterization of these mutants will be required in order to confirm this hypothesis. Evans et al. postulate that a deficiency in DNA repair could account for the production of multi-locus lesions by normally non-clastogenic mutagens such as UV and ethyl methansulfonate (EMS) (Evans et al., 1986). A DNA repair defect within Mutatect cells that would allow point mutations to be misrepaired in a fashion that produces strand breaks could account for the similarity seen between the mutants, regardless of the manner in which they were induced.

Since the mutational spectrum generated by the sequencing method was identical for all mutants analyzed, we can conclude that the presence of mutations which prevent expression of the hprt gene do not appear to be a direct result of the tumour environment, but may be due to intrinsic properties of the

Mutatect cells. However, it is important to note that the frequency of mutation induction varies for each mutant type. For example, the frequency of X-ray induced MN-11 mutants is ~5X higher (at 3 Gy) than the *in vitro* spontaneous mutation frequency (Wilkinson et al., 1995), and similarly, the mutation frequencies observed during *in vivo* growth are higher than those obtained *in vitro* (see section 3.1.5). Therefore, even though the treatments analysed may be generating the same types of mutations, they occur much more infrequently in the spontaneous mutants.

In conclusion, the results of the screening strategy are consistent with the suggestion that large-scale deletion mutations are induced in mutants of Mutatect cells. These large-scale mutations are evident not only in radiation and GTN-induced mutants, but also mutants generated spontaneously during *in vitro* and *in vivo* growth, although the spontaneous mutations occur at a lower frequency.

4. GENERAL DISCUSSION AND CONCLUSIONS

Mutagenicity and genetic instability within the Mutatect tumour model is correlated with an increase in neutrophil infiltration and iNOS activity. Reactive nitrogen and/or oxygen species are likely to be responsible for the mutagenesis seen in Mutatect tumours. Since previous work in our lab has shown nitric oxide to be capable of inducing large-scale deletions, the objective of my thesis project was to determine if this kind of mutation was arising during *in vivo* tumour growth. However, before characterization of the mutants could begin, additional information regarding the nature of the hprt marker gene was needed.

During development of the Mutatect cell lines, the X-linked hprt locus was genetically manipulated to allow for the sensitive detection of both large and small mutations. Previous indirect evidence suggested that the marker locus was heterozygous and that there were likely to be 3 copies of the hprt gene. To characterize the hprt genotype, I cloned and sequenced hprt cDNA to reveal that Mutatect cells contain 2 non-functional and 1 wild type gene. This is direct evidence of the heterozygous nature of the hprt locus.

The presence of 3 marker genes in Mutatect cells suggests that mutants will be tolerant of large multi-locus deletions, and makes this system a powerful tool for the investigation of these types of mutagenic events. However, the presence of 3 hprt genes also makes the molecular characterization of these mutations more difficult than in other systems. A strategy was required that would be able to distinguish the differences between the 3 genes (or gene

products) and allow us to detect mutations occurring in the wild type gene in the presence of two other mutated copies. The screening strategy I employed appeared capable of detecting mutations that prevented the expression of the wild type gene, as would be the case in large-scale deletions.

Analysis of a series of hprt$^-$ mutants using this screening method showed that the wild type cDNA sequence was absent from all of the hprt mutants studied. This suggests that hprt gene loss may account for a high proportion of mutant Mutatect cells. While this strategy does not prove the existence of large-scale deletions within Mutatect cells, it is consistent with this hypothesis. Future analysis of mutants involving quantitative multiplex PCR or FISH employing hprt specific probes may provide additional evidence to support the gene loss hypothesis. These methods would allow us to determine how many copies of the hprt gene are present in mutant clones (i.e., two copies versus three), and may also be useful in mapping the end points of any large deletions. As well, further characterization of the hprt locus of Mutatect cells at the DNA level may reveal other allelic variations that can be exploited to distinguish the 3 genes.

Even though the mutation spectrum (by this method) was the same for both spontaneous and induced mutants, the rate at which these mutations occur is much higher in the latter. Therefore, we can conclude that mutagenic factors present in the tumour environment promote the accumulation of mutations that prevent expression of the hprt gene.

In conclusion, this work has provided valuable input to some long-unanswered questions regarding the hprt marker locus in Mutatect cells. The

characterization of the 3 hprt mRNAs has allowed for mutants to be examined at the molecular level for the first time. Although not definitive, analysis of the mutants suggests that large-scale deletions may be induced by genotoxic factors present in the tumour environment. If future work proves this to be true, the evidence that inflammatory cells play a role in genomic instability and tumour progression will be strengthened.

References

Beckman,J.S. and Koppenol,W.H. (1996). Nitric oxide, superoxide, and peroxynitrite: The good, the bad, and the ugly. Am. J. Physiol. Cell Physiol. *271*, C1424-C1437.

Beltran,B., Orsi,A., Clementi,E., and Moncada,S. (2000). Oxidative stress and S-nitrosylation of proteins in cells. Br. J. Pharmacol. *129*, 953-960.

Birnboim,H.C. (1993). Extraction of high molecular weight RNA and DNA from cultured mammalian cells. Meth. Enzymol. *216*, 154-160.

Breimer,L.H., Nalbantoglu,J., and Meuth,M. (1986). Structure and sequence of mutations induced by ionizing radiation at selectable loci in Chinese hamster ovary cells. J. Mol. Biol. *192*, 669-674.

Breneman,J.W., Swiger,R.R., Ramsey,M.J., Minkler,J.L., Eveleth,J.G., Langlois,R.A., and Tucker,J.D. (1995). The development of painting probes for dual-color and multiple chromosome analysis in the mouse. Cytogenet. Cell Genet. *68*, 197-202.

Bruch-Gerharz,D., Ruzicka,T., and Kolb-Bachofen,V. (1998). Nitric oxide in human skin: current status and future prospects. J. Invest Dermatol. *110*, 1-7.

Burkhart-Schultz,K.J., Thompson,C.L., and Jones,I.M. (1996). Spectrum of somatic mutation at the hypoxanthine phosphoribosyltransferase (*hprt*) gene of healthy people. Carcinogenesis *17*, 1871-1883.

Burney,S., Caulfield,J.L., Niles,J.C., Wishnok,J.S., and Tannenbaum,S.R. (1999). The chemistry of DNA damage from nitric oxide and peroxynitrite. Mutat. Res. *424*, 37-49.

Chinault,A.C. and Caskey,C.T. (1984). The hypoxanthine phosphoribosyltransferase gene: a model for the study of mutation in mammalian cells. Prog. Nucleic Acid Res. Mol. Biol. *31*, 295-313.

Coleman,W.B. and Tsongalis,G.J. (1999). The role of genomic instability in human carcinogenesis
1. Anticancer Res. *19*, 4645-4664.

Dantzer,F., Schreiber,V., Niedergang,C., Trucco,C., Flatter,E., De La,R.G., Oliver,J., Rolli,V., Menissier-de Murcia,J., and de Murcia,G. (1999). Involvement of poly(ADP-ribose) polymerase in base excision repair. Biochimie *81*, 69-75.

DəMarini,D.M., Brockman,H.E., de Serres,F.J., Evans,H.H., Stankowski,L.F., Jr., and Hsie,A.W. (1989). Specific-locus mutations induced in eukaryotes (especially mammalian cells) by radiation and chemicals: a perspective
1. Mutat. Res. *220*, 11-29.

Dewyse,P. and Bradley,W.E. (1989). High-frequency deletion event at aprt locus of CHO cells: detection and characterization of endpoints. Somat. Cell Mol. Genet. *15*, 19-28.

Dugas,B., Mossalayi,M.D., Damais,C., and Kolb,J.P. (1995). Nitric oxide production by human monocytes: Evidence for a role of CD23. Immunol. Today *16*, 574-580.

Eizirik,D.L. and Leijerstam,F. (1994). The inducible form of nitric oxide synthase (iNOS) in insulin-producing cells
1. Diabete Metab *20*, 116-122.

Evans,H.H. (1994). Failla Memorial Lecture. The prevalence of multilocus lesions in radiation-induced mutants. Radiat. Res. *137*, 131-144.

Evans,H.H., Mencl,J., Horng,M.-F., Ricanati,M., Sanchez,C., and Hozier,J. (1986). Locus specificity in the mutability of L5178Y mouse lymphoma cells: the role of multilocus lesions. Proc. Natl. Acad. Sci. USA *83*, 4379-4383.

Fearon,E.R. and Vogelstein,B. (1990). A genetic model for colorectal tumorigenesis. Cell *61*, 759-767.

Felley-Bosco,E. (1998). Role of nitric oxide in genotoxicity: implication for carcinogenesis. Cancer Metastasis Rev. *17*, 25-37.

Gebara,M.M., Drevon,C., Harcourt,S.A., Steingrimsdottir,H., James,M.R., Burke,J.F., Arlett,C.F., and Lehmann,A.R. (1987). Inactivation of a Transfected Gene in Human Fibroblasts Can Occur by Deletion, Amplification, Phenotypic Switching, or Methylation. Mol. Cell. Biol. *7*, 1459-1464.

Grant, D. D. Mutations in the hypoxanthine phosphoribosyltransferase (hprt) gene in T lymphocytes from arthritis patients and in human B lymphoid cell lines exposed to nitric oxide-donating drugs. 1999. University of Ottawa.
Ref Type: Thesis/Dissertation

Graziewicz,M., Wink,D.A., and Laval,F. (1996). Nitric oxide inhibits DNA ligase activity - potential mechanisms for NO-mediated DNA damage. Carcinogenesis *17*, 2501-2505.

Hibbs,J.B., Jr., Taintor,R.R., Vavrin,Z., and Rachlin,E.M. (1988). Nitric oxide: a cytotoxic activated macrophage effector molecule [published erratum appears in Biochem Biophys Res Commun 1989 Jan 31;158(2):624]
1. Biochem. Biophys. Res. Commun. *157*, 87-94.

Ignarro,L.J., Fukuto,J.M., Griscavage,J.M., Rogers,N.E., and Byrns,R.E. (1993). Oxidation of nitric oxide in aqueous solution to nitrite but not nitrate: comparison with enzymatically formed nitric oxide from L- arginine. Proc. Natl. Acad. Sci. USA *90*, 8103-8107.

Isamat,M., Macleod,K.F., King,A., McEwan,C., and Melton,D.W. (1988). Characterization, evolutionary relationships, and chromosome location of processed mouse HPRT pseudogene. Somat. Cell Mol. Genet. *14*, 359-369.

Kadhim,S.A., Burns,B.F., and Birnboim,H.C. (1987). In vivo induction of tumor variants by phorbol 12-myristate 13-acetate. Cancer Lett. *38*, 209-214.

Keohavong,P. and Thilly,W.G. (1989). Fidelity of DNA polymerases in DNA amplification. Proc. Natl. Acad. Sci. USA. *86*, 9253-9257.

Kimura,H., Weisz,A., Kurashima,Y., Hashimoto,K., Ogura,T., D'Acquisto,F., Addeo,R., Makuuchi,M., and Esumi,H. (2000). Hypoxia response element of the human vascular endothelial growth factor gene mediates transcriptional regulation by nitric oxide: control of hypoxia-inducible factor-1 activity by nitric oxide
3. Blood *95*, 189-197.

Knudson,A.G., Jr. (1977). Genetics and etiology of human cancer
1. Adv. Hum. Genet. *8*, 1-66.

Loeb,L.A. (1991). Mutator phenotype may be required for multistage carcinogenesis. Cancer Res. *51*, 3075-3079.

Melton,D.W., Konecki,D.S., Brennand,J., and Caskey,C.T. (1984). Structure, expression, and mutation of the hypoxanthine phosphoribosyltransferase gene. Proc. Natl. Acad. Sci. USA. *81*, 2147-2151.

Melton,D.W., McEwan,C., McKie,A.B., and Reid,A.M. (1986). Expression of the mouse HPRT gene: deletional analysis of the promoter region of an X-chromosome linked housekeeping gene. Cell *44*, 319-328.

Murphy,M.P. (1999). Nitric oxide and cell death
1. Biochim. Biophys. Acta *1411*, 401-414.

Nathan,C. (1992). Nitric oxide as a secretory product of mammalian cells. FASEB J. *6*, 3051-3064.

Nguyen,T., Brunson,D., Crespi,C.L., Penman,B.W., Wishnok,J.S., and Tannenbaum,S.R. (1992). DNA damage and mutation in human cells exposed to nitric oxide in vitro. Proc. Natl. Acad. Sci. USA. *89*, 3030-3034.

Nowell,P.C. (1976). The clonal evolution of tumor cell populations. Science *194*, 23-28.

Phillips,E.N., Xia,F., Kelsey,K.T., and Liber,H.L. (1995). Spectra of spontaneous and X-ray-induced mutations at the *hprt* locus in related human lymphoblast cell lines that express wild- type or mutant p53. Radiat. Res. *143*, 255-262.

Podlutsky,A., Osterholm,A.M., Hou,S.M., Hofmaier,A., and Lambert,B. (1998). Spectrum of point mutations in the coding region of the hypoxanthine- guanine phosphoribosyltransferase (hprt) gene in human T-lymphocytes in vivo. Carcinogenesis *19*, 557-566.

Rincon-Limas,D.E., Krueger,D.A., and Patel,P.I. (1991). Functional characterization of the human hypoxanthine phosphoribosyltransferase gene promoter: evidence for a negative regulatory element. Mol. Cell Biol. *11*, 4157-4164.

Sandhu,J.K. and Birnboim,H.C. (1997). Mutagenicity and cytotoxicity of reactive oxygen and nitrogen species in the MN-11 murine tumor cell line. Mutat. Res. *379*, 241-252.

Sandhu,J.K., Haqqani,A.S., and Birnboim,H.C. (2000a). Effect of dietary vitamin E on spontaneous or nitric oxide donor-induced mutations in a mouse tumor model. J. Natl. Cancer Inst. *92*, 1429-1433.

Sandhu,J.K., Privora,H.F., Wenckebach,G., and Birnboim,H.C. (2000b). Neutrophils, nitric oxide synthase, and mutations in the Mutatect murine tumor model. Am. J. Pathol. *156*, 509-518.

Sanger,F., Nicklen,S., and Coulson,A.R. (1977). DNA sequencing with chain-terminating inhibitors. Proc. Natl. Acad. Sci. USA *74*, 5463-5467.

Schwartz,J.L., Ashman,C.R., Atcher,R.W., Sedita,B.A., Shadley,J.D., Tang,J., Whitlock,J.L., and Rotmensch,J. (1991). Differential locus sensitivity to mutation induction by ionizing radiations of different LETs in Chinese hamster ovary K1 cells. Carcinogenesis *12*, 1721-1726.

Steinitz,M. (2000). Quantitation of the blocking effect of tween 20 and bovine serum albumin in ELISA microwells. Anal. Biochem. *282*, 232-238.

Stout,J.T. and Caskey,C.T. (1988). The Lesch-Nyhan syndrome: clinical, molecular and genetic aspects. Trends. Genet. *4*, 175-178.

Szabó,C. and Ohshima,H. (1997). DNA damage induced by peroxynitrite: subsequent biological effects. Nitric Oxide *1*, 373-385.

Wang,S., Wang,W., Wesley,R.A., and Danner,R.L. (1999). A Sp1 binding site of the tumor necrosis factor alpha promoter functions as a nitric oxide response element
1. J. Biol. Chem. *274*, 33190-33193.

Wilkinson,D., Sandhu,J.K., Breneman,J.W., Tucker,J.D., and Birnboim,H.C. (1995). *Hprt* mutants in a transplantable murine tumour arise more frequently *in vivo* than *in vitro*. Br. J. Cancer *72*, 1234-1240.

Wink,D.A. and Mitchell,J.B. (1998). Chemical biology of nitric oxide: Insights into regulatory, cytotoxic, and cytoprotective mechanisms of nitric oxide. Free Radic Biol Med *25*, 434-456.

Wu,H., Sachs,R.K., and Yang,T.C. (1998). Radiation-induced total-deletion mutations in the human hprt gene: a biophysical model based on random walk interphase chromatin geometry. Int. J. Radiat. Biol. *73* , 149-156.

Yermilov,V., Rubio,J., and Ohshima,H. (1995). Formation of 8-nitroguanine in DNA treated with peroxynitrite in vitro and its rapid removal from DNA by depurination. FEBS Lett. *376*, 207-210.

Yuan,J. and Glazer,P.M. (1998). Mutagenesis induced by the tumor microenvironment. Mutat. Res. *400*, 439-446.

Yuan,J., Narayanan,L., Rockwell,S., and Glazer,P.M. (2000). Diminished DNA repair and elevated mutagenesis in mammalian cells exposed to hypoxia and low pH [In Process Citation]
1. Cancer Res. *60*, 4372-4376.

Zhuang,J.C., Lin,C., Lin,D., and Wogan,G.N. (1998). Mutagenesis associated with nitric oxide production in macrophages. Proc. Natl. Acad. Sci. U. S. A *95*, 8286-8291.

Zhuang,J.C., Wright,T.L., DeRojas-Walker,T., Tannenbaum,S.R., and Wogan,G.N. (2000). Nitric oxide-induced mutations in the HPRT gene of human lymphoblastoid TK6 cells and in Salmonella typhimurium. Environ. Mol. Mutagen. *35*, 39-47.

Appendix I

List of reagents and suppliers

Reagent Name	Supplier
Acrylamide	BioBasic Inc.
Advantage HF-2 polymerase mix	Clonetech
Agarose	Boehringer Manheim
Aminopterin	Sigma
Ampicillin	Boehringer Manheim
AmpliTaq DNA polymerase	Perkin Elmer
Autoradiography film (X-Omat Blue XB-1)	Kodak
Boric acid	BDH
Bromophenol blue	BDH
C57Bl/6 mice	Charles River Laboratories
CDTA (1,2-cyclohexanediaminetetraacetic acid)	Sigma
Chloroform	BDH
Diethyl pyrocarbonate (DEPC)	Acros
Dimethyl sulfoxide	Sigma
Dipotassium hydrogen orthophosphate (K_2HPO_4)	BDH
Disodium hydrogen orthophosphate (Na_2HPO_4)	BDH
Dithiothreitol (DTT)	Sigma
DNTPs	Amhersham Pharmacia
Dulecco's modified Eagle medium (DMEM)	Gibco
EDTA (ethylenediamine tetraacetic acid)	BDH
Ethanol	BDH
Ethidium bromide	Gibco BRL
Fetal calf serum	Medicorp
3 MM filter paper	Whatmann
Formamide	BDH
Formic acid	BDH
Glucose	Sigma
Glycerol	BDH
Glyceryl trinitrate (GTN)	Sabex
Hypoxanthine	Sigma
INVαF' One Shot competent cells	Invitrogen
Isopropanol	Commercial Alcohols Inc.
Ligation buffer	Invitrogen
Lithium chloride (LiCl)	BDH
Lysozyme	Boehringer Mannheim
Magnesium chloride ($MgCl_2$)	BDH
Microcon filters	Amicon
Oligo $(dT)_{12-18}$ primer	Amersham Pharmacia

[α-^{33}P] ddNTPs	Amersham Pharmacia
Phenol	BDH
Polyethyleneglycol 8000 (PEG)	BDH
Potassium acetate	BDH
Potassium chloride (KCl)	BDH
Potassium dihydrogen phosphate (KH_2PO_4)	BDH
Proteinase K	Merck
Ribonuclease A	Sigma
Rnasin ribonuclease inhibitor	Promega
Silicon oil	BDH
SOC medium	Invitrogen
Sodium acetate	J.T. Baker
Sodium citrate	BDH
Sodium dodecylsulfate (SDS)	BDH
Sodium hydroxide (NaOH)	Fisher
SuperScript reverse transcriptase	Gibco BRL
Syringes (3 c.c)	BDH
T4 DNA ligase	Invitrogen
Tetracycline	Sigma
ThermoSequenase polymerase	USB
Thymidine	Sigma
6-thioguanine (6-TG)	Sigma
Tissue culture plates (10 cm, 96-well)	Falcon
Tris-HCl	BDH
Trypan blue	Matheson Coleman & Bell
Tryptone	BDH
Tween-20	Sigma
Urea	BDH
Vent DNA polymerase	New England Biolabs
X-gal (5-bromo-4-chloro-3-indolyl-β-D-galactoside)	Vector Biosystems
Xylene cyanol	Sigma
Yeast extract	BDH

Appendix II

PCR and sequencing primers

Primer Number	Sequence (5'→3')	Position in cDNA	Expected Size of PCR Product (bp)
55	CCG GCT TCC TCC TCA GAC	position 39 exon 1 (forward)	872
151	CTG GGG ACG CAG CAA CT	position 910 exon 9 (reverse)	
188	GAT TAG CGA TGA TGA ACC AGG	position 114 exon 2 (forward)	296
189	CAT TAC AGT AGC TCT TCA G	position 409 exon 3 (reverse)	
190	CAT TAT GCC GAG GAT TTG G	position 166 exon 2 (forward)	sequencing primer

Position in cDNA refers to nucleotide position of primer's 5' end. Nucleotide numbering is based on the mouse hprt cDNA sequence published in genbank (J00423).